UNCLASSIFIED

AD NUMBER

AD527761

NEW LIMITATION CHANGE

TO

Approved for public release, distribution unlimited

FROM

Distribution authorized to U.S. Gov't. agencies only; Test and Evaluation; SEP 1973. Other requests shall be referred to Director, Naval Research Laboratory, Attn: 1221-1, Washington, DC 20375.

AUTHORITY

NRL Code/5309 memo dtd 20 Feb 1997

THIS PAGE IS UNCLASSIFIED

UNCLASSIFIED

AD NUMBER	
AD527761	
CLASSIFICATION CHANGES	
TO	
unclassified	
FROM	
secret	
AUTHORITY	
December 31, 1993 IAW document markings.	

THIS PAGE IS UNCLASSIFIED

HF Ground-Wave Backscatter from Surface Targets (Phase B - San Clemente Island)

[Unclassified Title]

ROBERT W. BOGLE AND LEONARD S. WAGNER

Systems Research Staff
*Radar Division*

September 1973

NOV 7 1973

DDC CONTROL
NO. 32749

NAVAL RESEARCH LABORATORY
Washington, D.C.

SECRET-NOFORN

NATIONAL SECURITY INFORMATION

Unauthorized Disclosure Subject to Criminal Sanctions.

CONTENTS

DDC CONTROL
NO. 32749

HF GROUND-WAVE BACKSCATTER FROM SURFACE TARGETS
(Phase B - San Clemente Island)
(Unclassified Title)

ABSTRACT

(SNF)   Measurements of surface-vessel wakes have been made with an experimental HF radar. The experimental program was conducted at San Clemente Island in deep ocean areas. The radar was provided with considerable flexibility in frequency, range and azimuth and an on-site digital processor was used to provide near real-time spectral analyses. Preliminary results indicate that wakes are clearly distinguishable from the clutter produced by a nominal sea. Examples are given. Analysis of effective wake cross-section as a function of vessel speed and size and as a function of sea conditions are proceeding.

I. INTRODUCTION (U)

(S) In 1955, D. D. Crombie (1) provided an explana-
tion of the resonant Bragg scattering from the sea. The
theory of resonant scattering has been developed by D. E.
Barrick (2) and others. This theory, which has since been
thoroughly verified by numerous experiments, invokes the
principle of constructive electromagnetic scattering from
successive sea surface waves which are coherent over a
nominal distance. More recently Crombie (3) suggested the
possibility that ship's wakes would produce an effective
Bragg backscatter which is distinguishable from the sea.
Such a possibility would be of great significance in the
detection of surface targets by HF radars and on this basis
Project NONESUCH was designed to experimentally explore the
detectability of wakes with a flexible HF system.

(SNF) The qualitative question of detectability was
established in a series of preliminary experiments con-
ducted at the Salton Sea in early 1972 under conditions of
dead calm water (4). The equipment used at that time was
somewhat rudimentary but the results of the experiments
established unmistakably that wakes of an exceedingly small
amplitude produced an effect which was clearly discernible
to an HF radar. Furthermore, experimental results were
found to fit predicted theory in the frequency and doppler
domain. The experiments which were subsequently performed
under deep ocean conditions have been concerned with the
critical questions of radar cross-section as a function of
vessel size and velocity, and more significantly, the effect
of nominal sea in masking the wake backscatter and the
critical factor of wave saturation. The latter effect
could reasonably be expected to suppress or damp the wake
itself under sufficiently disturbed sea conditions.

(U) Preliminary results from these experiments are
discussed here, together with a description of some of the
details of the equipment and the manner in which the tests
were conducted.

(C) The experiment and the radar were designed to
provide great flexibility in the choice of significant
operating parameters and their sequencing. An on-site
general purpose computer was included and provided with
sufficient software to allow real and near real-time pro-
cessing, including fast Fourier transforms. As a conse-
quence of this system flexibility, it was possible to
expand the program of data acquisition to include measure-

ments of sea scatter under various conditions as well as aircraft dynamic cross-section. Both of these were done for a wide range of radio frequencies. The results of these experiments will be discussed in succeeding papers.

(U) In addition, measurements of surface-current velocities were made in cooperation with the Scripps Institution of Oceanography.

II. BACKGROUND (U)

(U) A Kelvin wake is a traveling disturbance on the surface of the sea produced by a moving pressure distribution, as from a boat, on or below the surface of the water. The phenomenon has received considerable attention over the last century, Lord Kelvin (5) and T. H. Havelock (6) being among the earlier contributors.

(U) The visible wake consists of a wave pattern which appears to trail, but move along with, the boat and which is confined to a triangular sector subtending an angle of approximately 38° as illustrated in Figure 1. A simple physical explanation of the wake geometry is given by Tricker (7). Inspection of the actual wave structure in the wake shows that it consists of two distinguishable groups, a transverse and a cuspidal wake. (The latter is much more obvious to the eye.) The transverse wake fills most of the triangular wake area and has phase fronts which are approximately normal to the boat trajectory. The cuspidal wake is spatially confined to the edges of the triangular region and has its phase fronts aligned at an angle of approximately 54.5° to the boat trajectory. Studies of the Kelvin wake have indicated that the transverse wake amplitude decays as $(D)^{-\frac{1}{2}}$ and that the cuspidal wake decays as $(D)^{-\frac{1}{3}}$ where D is distance behind the boat.

(U) The disturbance created by the water displacement due to a ship consists of a superposition of water waves of different wavelengths traveling in different directions. Those waves which comprise a wake are water waves whose phase velocity and directions of travel are such that they are reinforced by the disturbance of the ship at all points of its space-time trajectory. This necessarily limits a wake to that set of water surface waves whose phase velocity is equal to the projection of the boat velocity along the direction of their travel

$$\text{i.e.} \qquad V_\phi = V_s \cos \theta \qquad\qquad (1)$$

where V_ϕ is wave phase speed

V_s is ship speed

θ is the wave propagation direction relative to ships heading.

(U) Since a wake is comprised of a special set of water waves they necessarily obey the same dispersion relation as ordinary waves

$$\omega = \sqrt{gk} \qquad \text{(deep water case) (2)}$$

where g is the acceleration of gravity at the Earth's surface, k is water wavenumber, and ω is frequency of the water waves in rad/sec. The expression for phase velocity resulting from this dispersion relation is

$$V_\phi = \frac{g}{k} \qquad\qquad (3)$$

and the group velocity can be shown to be always half the phase velocity.

(U) Assuming HF backscatter to result from a Bragg mechanism, the radar frequency for resonant interaction with the wake will be dependent upon the radar viewing angle off the boat trajectory. Making use of the Bragg criteria $\lambda = \Lambda/2$, where λ is radar wavelength and Λ is water wavelength, and of equations (1) and (3) one can show that the radar frequency for resonant interaction f_{res} is given by

$$f_{res} = \frac{gc}{4\pi(V_s \cos \theta)^2} \qquad\qquad (4)$$

where c is the velocity of light in vacuum and all other quantities are as previously defined.

(SNF) The visibility of wake in the presence of strong background clutter due to the ambient wind-driven sea depends upon its highly organized structure. Within a coherent patch of wake the backscattered electric field adds arithmetically as opposed to a power addition that one might expect from a random superposition of resonant wavelets. The visibility of a wake in a realistic sea environment clearly depends upon the relative coherence lengths of wake

and ambient sea and also upon the effect of wave-wave inter-
action upon wake structure and coherence length.

(U)   The location for the Project NONESUCH experiments
is the western shore of San Clemente Island, approximately
60 miles southwest of Long Beach.   The off-shore waters
deepen rapidly and are fully exposed to the Pacific.   Since
the NONESUCH experiment was concerned with target models,
ranges of operation were constrained generally to within
40 km (90 km in the case of some aircraft measurements),
and the ground-wave propagation mode was chosen, thereby
providing freedom from ionospheric spectral disturbance.
The western side of San Clemente Island slopes gently to a
flat plain of low elevation and is therefore ideal for the
deployment of antennas suited to the ground-wave mode.
Figure 2, a map of San Clemente Island shows the general
location of the radar and includes idealized antenna pat-
terns produced by both the transmitting and receiving
arrays.   Figure 3 and Figure 4 illustrate the site and the
trailer vans used to house the electronic and computer
equipment, and Figure 5 shows the two-bay log-periodic
transmit antenna.   Figure 6 is a view of the receiving
array.   Details of these are discussed below.

III. DESCRIPTION OF THE EQUIPMENT (U)

(C)   The equipment used in the experiments consists of
a high frequency ground-wave radar optimized for observing
sea scatter.   The system consists of a receive array control
unit, a timing and frequency control unit, a receiver,
transmitter, and on-line computer for signal processing.   A
moderately wide transmitting antenna beam provides area
coverage for a dual beam receiving array of narrower beam
width.   The receiving beam centers lie on azimuths of 240°
and 270° true.   They are switched alternately by a timing
logic which also triggers pre-selected radio frequencies
and selectable range gates.

(S)   Figure 7 shows the radar system diagrammatically.
The timing and frequency control unit is designed for great
flexibility to accommodate a wide range of formats.   The
time base can be any integral multiple of 10 microseconds
up to one second.   Up to 99,999 different frequencies can be
programmed by a pinboard arrangement for transmission in
time sequence.   The control logic unit drives a frequency
synthesizer whose output frequency can be changed on a
pulse-to-pulse basis.   The synthesizer frequency determines

the frequency of the radar pulse transmitted and also tunes
the receiver to the backscatter from the pulse transmitted.
Since the same frequency drives both the transmitter and the
receiver, frequency coherence is maintained to allow FFT
processing of the individual returns from the different fre-
quencies transmitted in the 2 - 20 MHz frequency range.

(U) A general purpose computer is utilized to format
the data and perform spectral analyses in real-time. The
processor has a 32K memory, 16 bit words, a 475,000 word
disc storage, a 12 bit analog to digital converter, and a
45 ips magnetic tape unit. The unit has been programmed to
calculate as many as 100 data channels simultaneously with
the FFT. However it is limited to a maximum of approxi-
mately 600 input words per second; with 100 channels a
maximum spectral analysis bandwidth of 3 Hz is possible.
Fewer channels allow wider bandwidths. A memory oscillo-
scope is utilized to display a few selected data channel
outputs in real-time for purposes of on-line monitoring of
the experiment in progress. A Calcomp drum plotter and
data print-out provide outputs in non real-time. The capa
bility to inspect quantitative results shortly after a test
run has greatly aided the optimization of experiments.

(U) The transmitting antenna is an array of two TCI
Model 513 vertically polarized log periodic curtains
arranged in a vee with the apex forward to achieve a beam-
width of approximately 65 degrees. This antenna is placed
over a large ground screen which stops just short of the
water's edge. The power gain of this antenna varies from
about 10-14 dB above isotropic, depending upon frequency.

(U) The receiving antenna consists of a linear broad-
side array of 13 vertical monopoles. Either 7 or 8 of these
monopoles are selected by the switching logic to form two
beams approximately 15 degrees wide separated from each
other by 30 degrees. Figure 8 shows examples of measured
patterns of the left and right receiver beams relative to
the transmitter antenna beam at 9.3 MHz. These beams are
formed by a number of fast switches and phasing lines in
the beam-forming and switching unit driven by the timing
and frequency control unit. The monopoles are 25 ft. long
and are roughly matched to the transmission lines by 600-
to-50 ohm transformers which tend to smooth the response
with frequency over the band. Gains vary between -20 and
+5 dB. The elements are placed over a conducting ground
mat with radials extending from each antenna element into
the water.

(U)   The receiver noise figure is 15 dB or less.   The
in-band IM products are down a minimum of 60 dB from the
principle components when they are introduced at the
receiver front end at a level of -60 dBm corresponding to
the maximum output level.   The out-of-band IM products were
not observable above the noise level whose peak values were
40 dB below the in-band signal, f, when it was introduced
into the receiver at -56 dBm and the signal at 2f was intro-
duced at a level of +3 dBm.   With the 2f signal at -37 dBm
the product signal was below the noise level peaks, 60 dB
below the in-band signal.

(U)   The signal-to-noise peaks of the transmitter pulse
itself appear to be of the order of 65 dB (72 dB to mean
noise values) when using 27 dB of processing gain with the
nominal 50 microsecond pulse length and the corresponding
receiver bandwidth of 20 kHz.

(U)   The filter bandwidths of the receiver at the inter-
mediate frequencies have about a 3.5:1 ratio between the 60
to 6 dB bandwidths.   There are some sidelobes in the time
domain, but they are a minimum of 25 dB down for the first
one.   The receiver bandwidths are a nominal 10, 20, or 50
kHz to accommodate transmitter pulse lengths of 100, 50, or
20 microseconds respectively.   A Gaussian filter is employed
in the transmitter pulse-forming circuits so the tails of
the pulses extend considerably beyond these lengths.   Peak
pulse powers extend up to approximately 70-80 kw.

(U)   The predicted values of beamwidth for the trans-
mitter and both receiver beams were verified.   Also the
true bearings of the receive-beam maxima were established
with reference to the output of a supporting X-band tracking
radar which was used throughout the experiments to guide
and to track the target sources used (e.g. surface boats and
aircraft).   Received power was calibrated by injection of a
known calibration signal into the recorded data while radar
cross-section measurements were being made.   Transmitted
power was determined from the product of transmitter output
current, measured with calibrated ammeters, and impedance of
the transmit antenna as determined by exhaustive measure-
ments of the antenna impedance made on site for the band of
frequencies used.   Pulse duty factor was determined by inte-
gration of transmitter pulse shapes as displayed and photo-
graphed with a sampling signal on an oscilloscope.

IV. CALIBRATION (U)

(U) Considerable effort was devoted to calibration of the NONESUCH system by a variety of techniques. Extensive antenna pattern and gain measurements were made with a calibrated signal source which was moved in precisely determined arcs offshore from the site at a range of two n.mi.

(U) System sensitivity parameters were determined by a comparison of several calibration methods. First, the ensemble of measured system parameters, including $G_R G_T$, P_R, P_T and range (as measured with the X-band radar) and losses were inserted in the radar equation. The latter included system cable losses, excess ground-wave loss, surface roughness loss and, when applicable, loss due to the dynamic response of the receiver. In situ measurements of a calibrated monopole, placed in the sea at a precise range and on antenna beam center were made. This monopole, shown in Figure 9 consists of an adjustable whip antenna mounted in a small aluminum boat and grounded through a crystal-controlled switch. The cross-section of this system was measured earlier against the carefully calibrated NRL MADRE radar and found to produce a measured cross-section which matched the theoretically predicted value (at approximately 10 MHz) to within about one dB. At San Clemente Island the monopole cross-section was measured at six sample frequencies across the system band. (At 3.25 MHz a different, structured mast was used with a somewhat larger vessel.) The results of these measurements were used as a second, independent measurement of antenna gain product.

(U) A third input to the sensitivity calibration was provided by J. M. Headrick of NRL, who used the backscatter from a fully developed sea as a reference cross-section (8).

(U) Figure 10 plots the system sensitivity in terms of antenna gain product. All uncertainties in the various measurements are incorporated in the data points shown; these include interpretation of the antenna pattern measurements, uncertainties in P_T and some indeterminacy in a knowledge of the propagation losses. On the basis of considered judgment, it is felt that the accuracy of the smoothed curve is within ±2 dB. The shape of the gain product curve is a function of (a) the mismatch loss of the receive antennas, (b) an anomaly in the gain of the transmit antenna at 12.1 MHz (indicated by the dip at that frequency)

7

and (c) a change of gain at the frequencies where the
switching logic inserts or removes a receive antenna element
(indicated by the discontinuities in the curve).

V. SUPPORTING INSTRUMENTATION AND SURFACE CRAFT (U)

(U) The San Clemente Island test facility is operated
by the Naval Undersea Center (NUC). As part of this sup-
port an M-33 X-band tracking radar, converted for instru-
mentation provided precise positioning for all material
targets (boats, ships and aircraft) and post-tes. records
of their positions as a function of time. This radar
source provided accurate metric data for both target tra-
jectories and for the antenna pattern measuremerts. The
primary work craft used for wake generation and for towing
the NONESUCH Monopole was a torpedo recovery boat (TRB) of
50 tons displacement and 15 knots maximum speed.

(SNF) A prime objective of the NONESUCH experiment is
the evaluation of wake detectability in the presence of
various sea states. To provide a quantitative and contem-
porary measure of this quantity, an instrumented wave buoy
was moored in the test area at an offshore range of approxi-
mately 15 miles. This buoy transmits a telemetered signal
to shore instrumentation which in turn produces a precise
analog representation of the ocean wave displacement for
frequencies between 0.03 and 0.6 Hz. The output from this
system was recorded in three ways. The instrument produces
a continuous calibrated analog chart. NRL provided in
addition, a digital recorder and A/D converter to allow
later spectral analyses. Finally, a Ubiquitous wave
analyser and averager was used to produce energy density
spectra in near real-time.

(SNF) The radar measurement experiments examined wakes
produced by the TRB mentioned above, a DD (destroyer and a
DE (destroyer escort). Various velocities were used. To
date most of the data has been taken for radial courses.

VI. EXPERIMENTAL RESULTS (U)

(SNF) At the time of this reporting, preliminary
results show positive evidence of clearly detectable wakes
produced by even relatively small surface crafts. The wake

cross-sections to be shown are all the result of measurements of the normal view of the transverse Kelvin wake. Variation of cross-section or signal-to-clutter for crossing courses is yet to be examined. The relation of wake cross-section to the physical characteristics of the wake is under investigation. Furthermore, the effect on wake cross-section of clutter masking and wake suppression by disturbed sea conditions is under analysis and will be reported at a future date.

(SNF) The experimental procedure for producing these measurements was as follows. A wake-generating vessel (typically a TRB), a velocity and a course would be specified prior to a run. The boat would be vectored to a starting point by the X-band radar with steering headings given by voice radio to the helmsman. The starting point would generally be selected so as to produce a wake of finite but nominal length (with reference to the radar range gate). The run would be initiated by radio command from the NONESUCH control site for purposes of time coordination. Following this the tracking radar would provide guidance and position reports by voice radio.

(SNF) Using a relatively high radar frequency (e.g. 9 MHz), initial measurements of boat speed would be made at NONESUCH and corrections made to the boat speed via recommended changes of engine speed. Typically, 40 radar frequencies, spaced at 50 KHz intervals would be transmitted but because of the sensitive relationship of resonant wake doppler frequency on boat speed, some care was required to adjust it into band.

(SNF) Continued monitoring of the "velocimeter" (high frequency doppler channel) was done to assure that the boat speed, hence wake pattern, was as constant as possible. (It was observed that the TRB's could hold surprisingly constant speed while heading into the prevailing on-shore seas; when running with the sea, however, a surf-board effect produced significant variation of the speed.)

(S) The data are presented generally in two forms. In the first of these, an isogrammetric presentation plots successive doppler spectra with time proceeding "back" into the plot. The data have been normalized against the radar's calibrated sensitivity so that the vertical ordinate is proportional to dB above one square meter (dBsm) of effective

radar cross-section. The baseline of the spectrograms is set to exactly one square meter, i.e., 0 dBsm.

(U) The width of the spectral data is shown as minus (left) to plus 0.5 Hertz (i.e., with zero doppler off-set at the center). In the third dimension, since the time interval (time to average the desired number of samples) was constant, time can be interpreted as distance.

(SNF) Each of the isograms shows both the retreating sea return and the superimposed wake return when present on the left, and the advancing sea return on the right. The nature of the prevailing sea west of San Clemente Island is such that the advancing sea resonant line is generally the larger.

(SNF) The second form of presentation is a plot of peak wake cross-section (in the range gate) as a function of time. The measured cross-section is shown for several adjacent (50 KHz spacing) frequencies. The samples have been selected to illustrate the wake resonant frequency and the spectra from two or three adjacent frequencies. These plots provide a qualitative demonstration of the sharpness of the effect. They also establish the fact that the cross-section of the boat itself is small compared to that of the wake.

(SNF) The experimental format on the night of 7 December 1972 involved the use of a U. S. Navy destroyer (DD) which executed a radial course at a speed of 13.5 knots on a bearing of 240° between ranges of 4,000 and 30,000 yards. For that speed, the resonant radar frequency was calculated to be approximately 5 MHz. A twenty frequency format was chosen for the system with twelve frequencies grouped between 4.5 and 6 MHz. Additional frequencies were located elsewhere in the 2 - 20 MHz band to look for second-order and non-linear effects. One or two high frequencies, for which no resonance was anticipated, were used for the measurement of boat doppler. Range gates having a width of 7.5 km (to the 3 dB points) and centered on 15 and 22.5 km were used.

(S) Figure 11 is an isometric plot of the ship doppler spectra made for a radar frequency of 9.933 MHz. The shape of the range-dependent return typifies the $\cos^2$ shape of the

transmitter pulse. The X-axis represents doppler frequency and the oblique axis is a time axis with appropriate annotations. The vertical axis represents cross-section in dBsm for a target located at the center of the range gate. The floor of the plot represents a target cross-section of $1 m^2$ (0 dBsm) and the vertical axis of the original plot was adjusted to be 10 dBsm per large division. The effective cross-section of the ship at this frequency was judged to be 34 dBsm.

(SNF) Figure 12 is an isogram at a radar frequency of 4.543 MHz and covering the same time period. In this figure the feature at -0.22 Hz represents the recede resonant line. The threshold for plotting is a cross-section of $1 m^2$ as in the preceding figure. A large division of the vertical scale represents 10 dB. In this figure it is notable that a large enhancement occurs during the time of the boat transit through the range gate but disappears when the boat leaves the gate. It is also worth noting that during this experiment the sea approach resonant line is of the order of 15 dB greater than the recede line. During the course of this experiment, wave heights of the order of 3 to 4 feet with occasional 5 foot swells were measured with the wave buoy.

(SNF) Figures 13, 14 and 15 are isograms of the same event at frequencies of 4.933 MHz, 5.033 MHz and 5.113 MHz showing a sustained enhancement after the boat's disappearance from the range gate. The resonant effect appears to maximize at a frequency of 5 MHz which is precisely the frequency at which the resonance was anticipated. In these and all subsequent isograms the floor of the plot and the vertical scale will be the same as defined for the preceding isograms.

(SNF) Figure 16 is a time profile of backscatter cross-section for the event described in the preceding figures. The frequency of 9.933 MHz is included to define the limits of the range gate. It is clear from this plot that a distinct enhancement of the recede clutter line is produced by the presence of wake in the range gate. The magnitude of the enhancement is between 15 and 20 dB on frequencies of 4.933 and 5.033 MHz.

(SNF)   Figures 17 through 26 show similar enhancements on different days using the much smaller TRB operating at approximately the same boat speed. Sea conditions were about the same for all three events but this result must be confirmed by a more exhaustive perusal of the surface height measurements made by the Waverider buoy. Judging from the amplitude of the ambient sea clutter it appears that the roughest seas were encountered on the night of 7 December 1972 and that the mildest sea conditions were encountered on the day of 16 January 1973. It also appears that the largest wake cross-section was encountered on the 16 January event.

VII. CONCLUSION (U)

(SNF)   Evidence of the detectability of surface wakes by a coherent HF radar for some sea conditions has been presented. Further analysis and more experimentation will be required to establish the limits of this detectability for crossing courses of increasing aspect and for limiting conditions of sea state. It is expected that experimental evidence on hand from the NONESUCH tests performed to date will permit an evaluation of effective cross-section as a function of hull displacement and ship velocity. Questions of cross-section coefficient as a function of wake amplitude and effective wake area will also be explored.

(SNF)   With regard to wake cross-section coefficient, particularly by reference to generally accepted values of sea cross-section coefficient, a note of caution is in order. The wake cross-section (in dBsm) depends upon the area of the sea which was within the spatial resolution cell of the radar. For the data presented here, it is possible that the effective wake area was significantly smaller than this resolution cell. Examination of further data will be required to resolve this point. Of equal importance is the quantitative question of the possible augmentation of an otherwise "saturated" sea by a wake of long coherence length. (As a matter of tactical significance, of course, the synoptic probability of a saturated sea diminishes for low radio frequencies, i.e., high velocity vessels.)

VIII. REFERENCES (U)

1. D. D. Crombie, "Doppler Spectrum of Sea Echo at 13-56 Mc/s (U)", Nature, 175, 681 (1955), UNCLASSIFIED.

2. D. E. Barrick, "First Order Theory and Analysis of MF/ HF/VHF Scattering from the Sea (U)", IEEE Trans. on Antennas and Propagation, Vol AP 20, 2-10 (1972), UNCLASSIFIED.

3. D. D. Crombie, "HF Back Scatter from a Ship's Wake (U)", Procs. MAYBELL Technical Workshop, (May 1970), SECRET.

4. R. W. Bogle, L. S. Wagner, "HF Ground-Wave Backscatter From Surface Targets (U), (Phase A - Salton Sea)", NRL Memorandum Report, in publication, SECRET.

5. W. Thompson (Lord Kelvin), "On the Waves Produced by a Single Impulse in Water of Any Depth or in a Dispersive Medium (U)", Proc. Royal Soc., 40, p 80 (1887), UNCLASSIFIED.

6. T. H. Havelock, "Ship Wakes: The Calculation of Wave Profiles (U)", Proc. Royal Soc., A, 1-13 (1931), UNCLASSIFIED.

7. R. A. R. Tricker, "Bores, Breakers, Waves and Wakes (U)", American Elsevier, N. Y. (1964), UNCLASSIFIED.

8. J. M. Headrick, D. E. Barrick, "Some Features of Sea Echo at HF", Proc. of OHD Tech. Rev. Mtg., May 1973, UNCLASSIFIED.
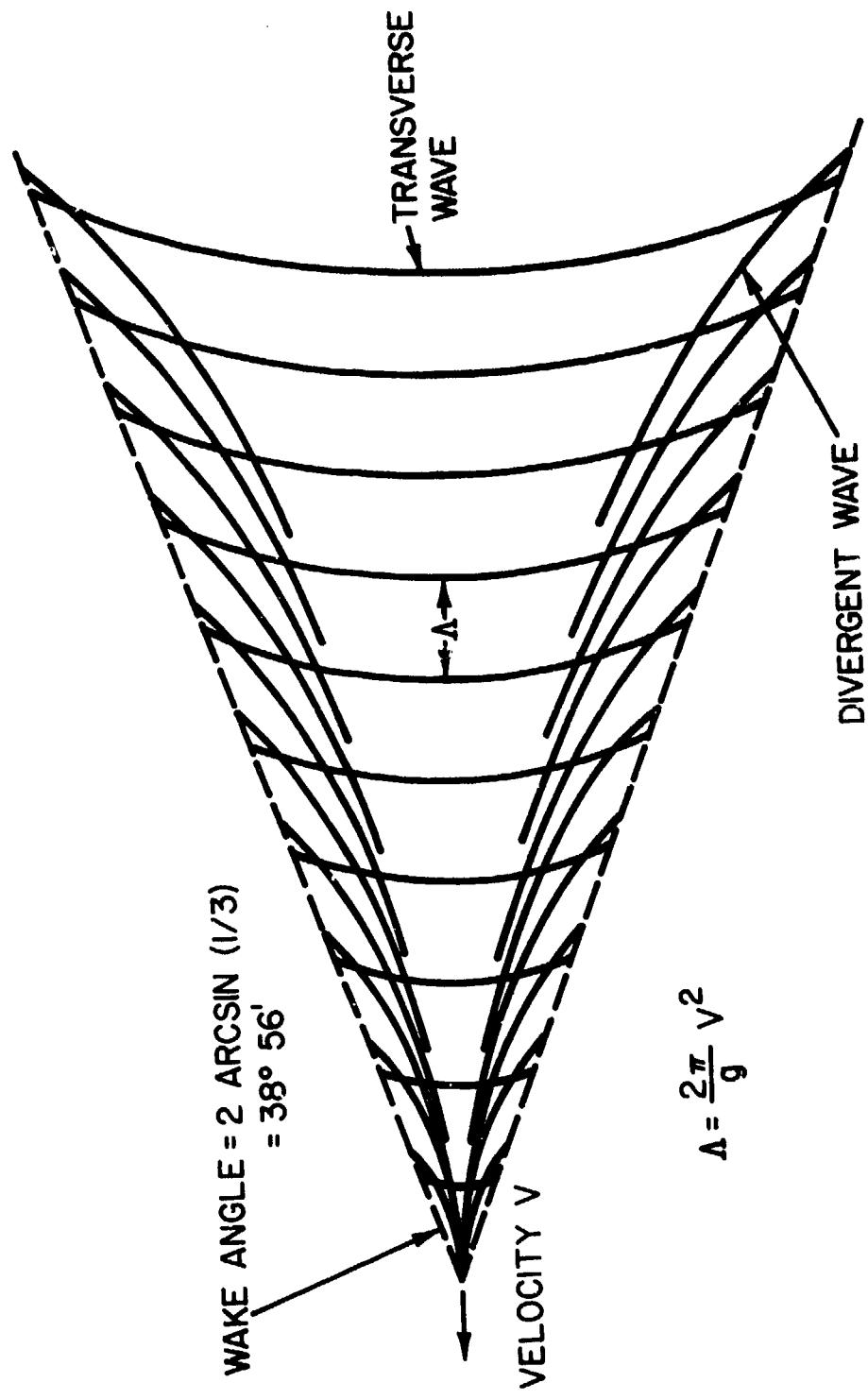
(S) Fig. 1 – Kelvin wake geometry

WAKE ANGLE = 2 ARCSIN (1/3)
= 38° 56'

TRANSVERSE WAVE

DIVERGENT WAVE

VELOCITY V

$\Lambda = \frac{2\pi}{g} V^2$
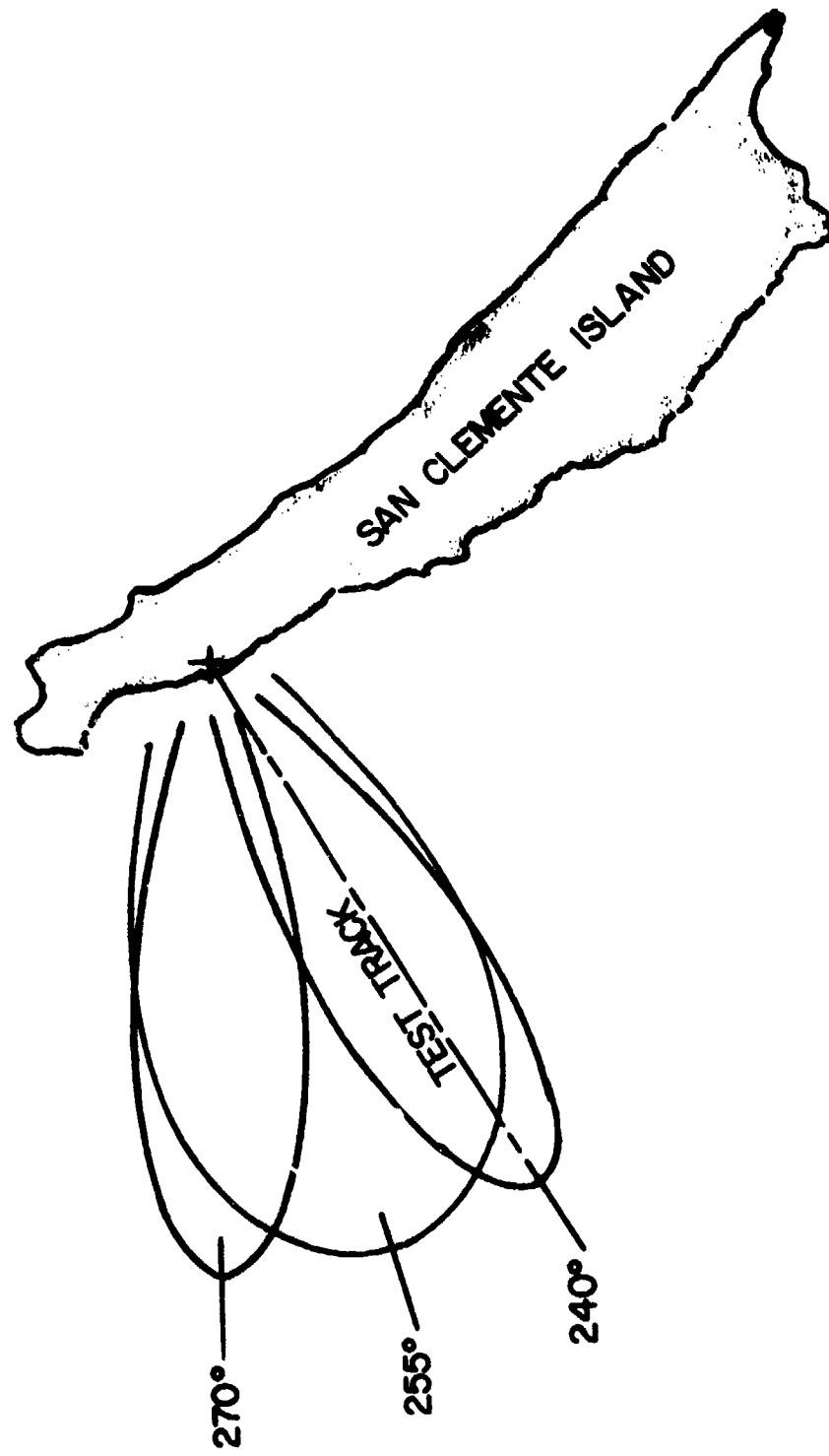
(S) Fig. 2 – Geometry of the NONESUCH test track

(S) Fig. 3 – Air view of the radar site

(S) Fig. 4 - Receiver and data processing trailers (foreground); high power transmitter trailer (left background)
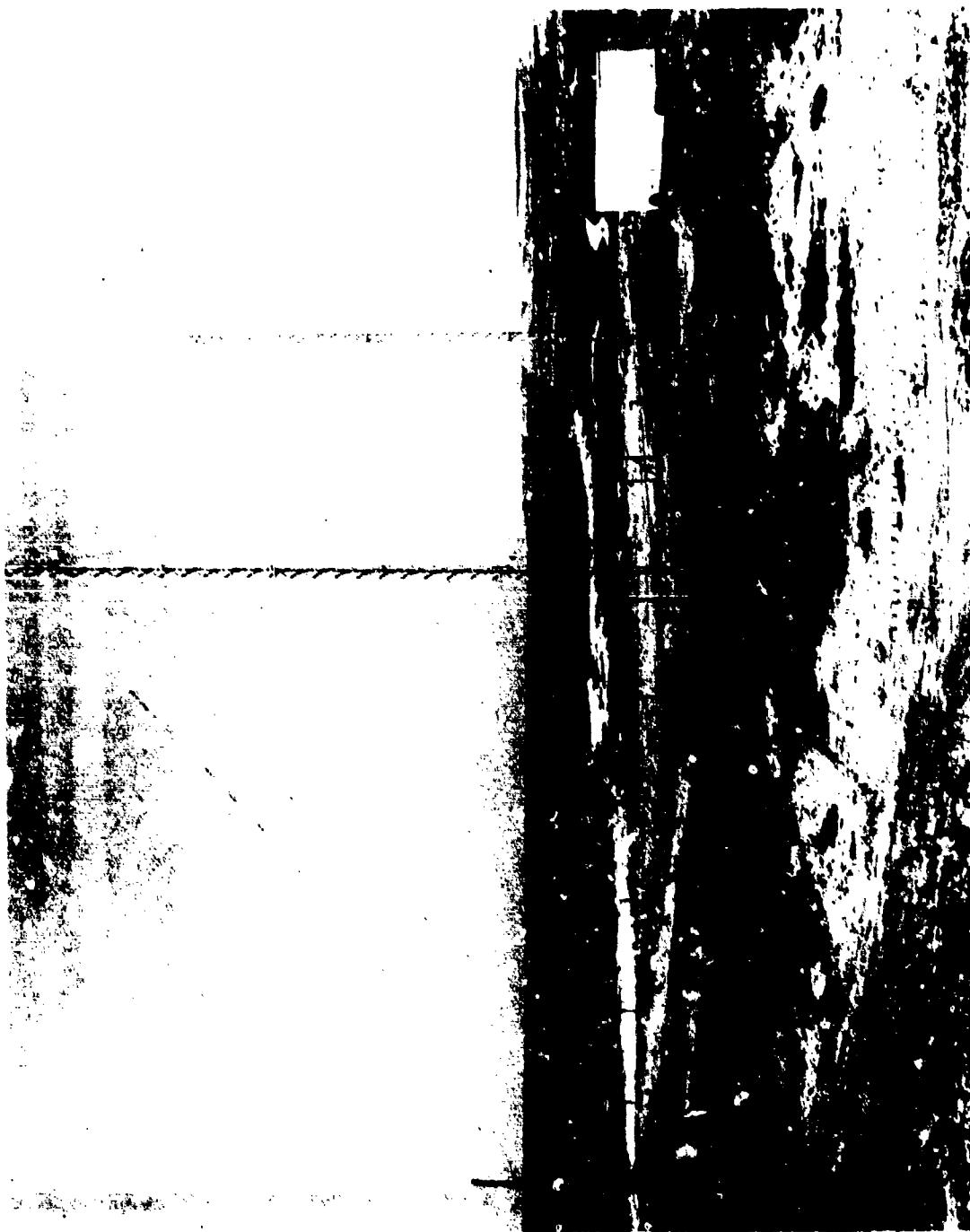
(S) Fig. 5 - The NONESUCH log-periodic curtain transmit array

18
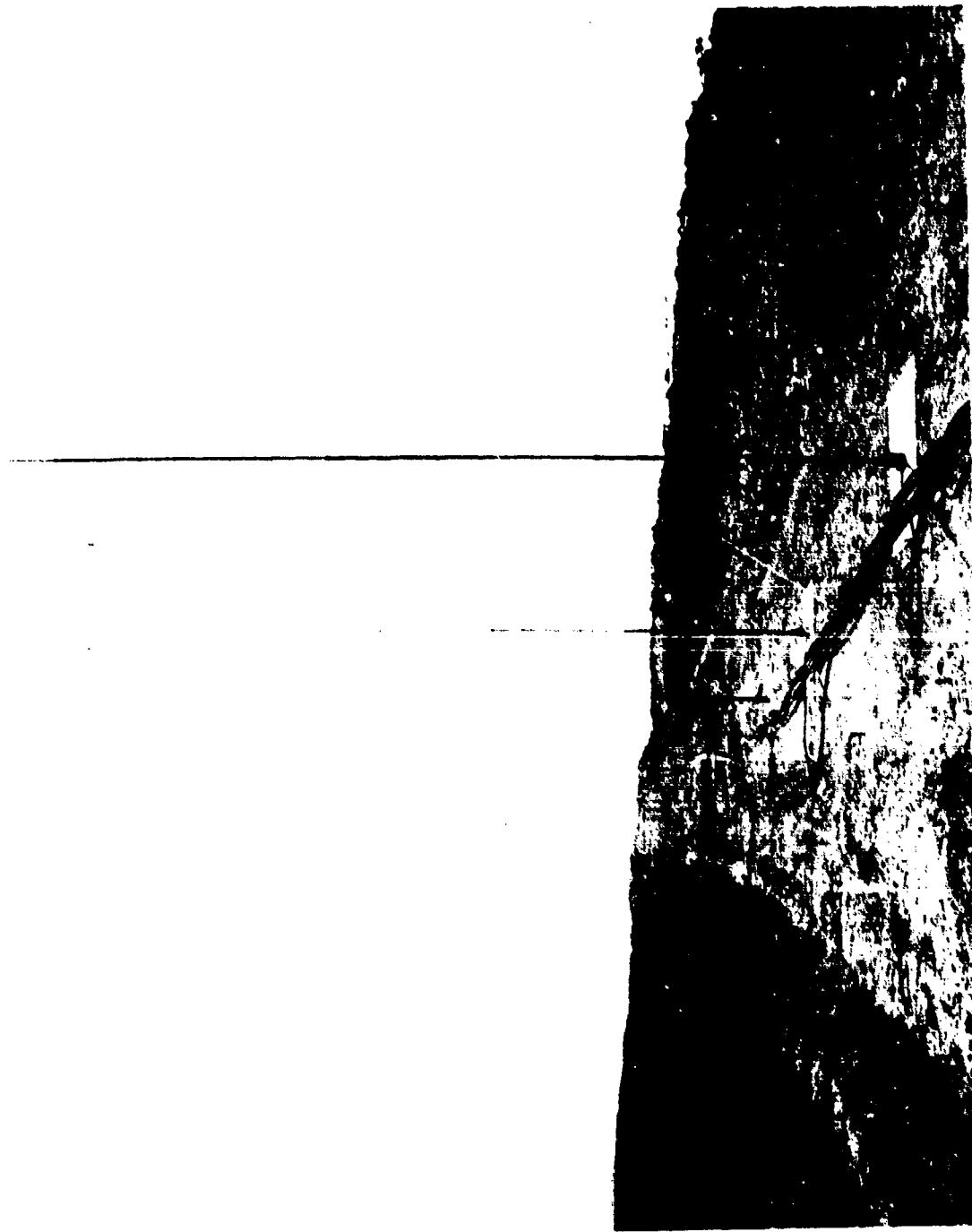
(S) Fig. 6 – The NONESUCH receive antenna array
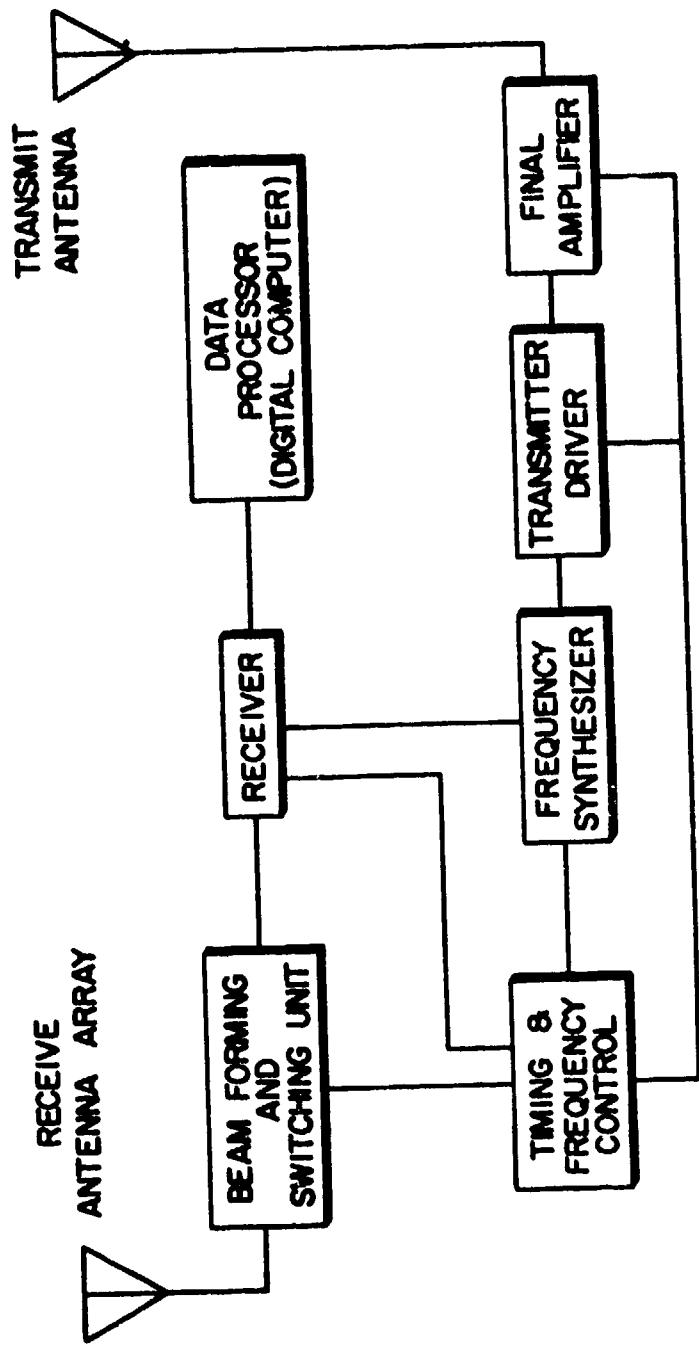
(S) Fig. 7 – Block diagram of the coherent frequency agile NONESUCH radar system
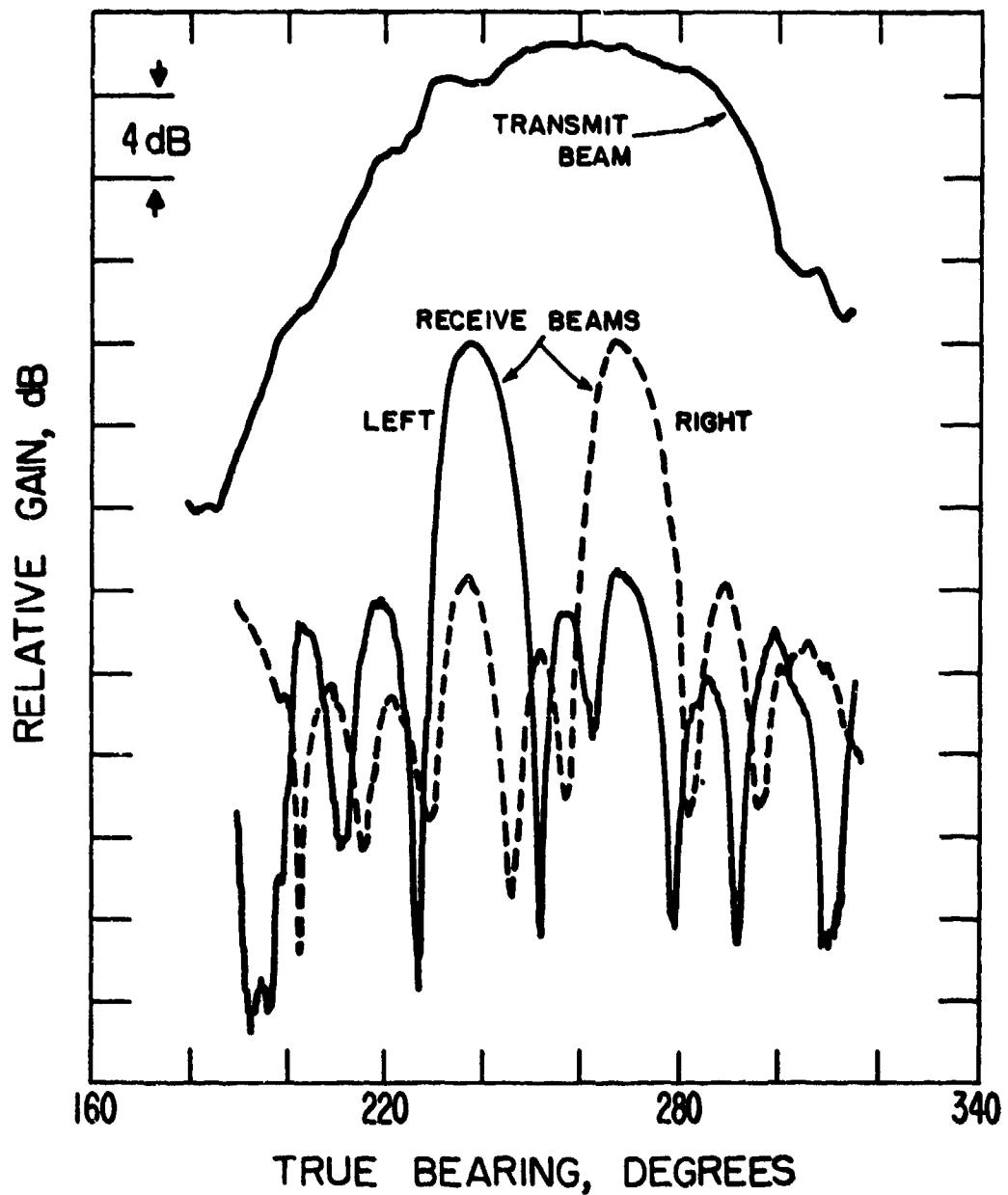
(S) Fig. 8 – Typical transmit and receive antenna patterns (9.3 MHz)
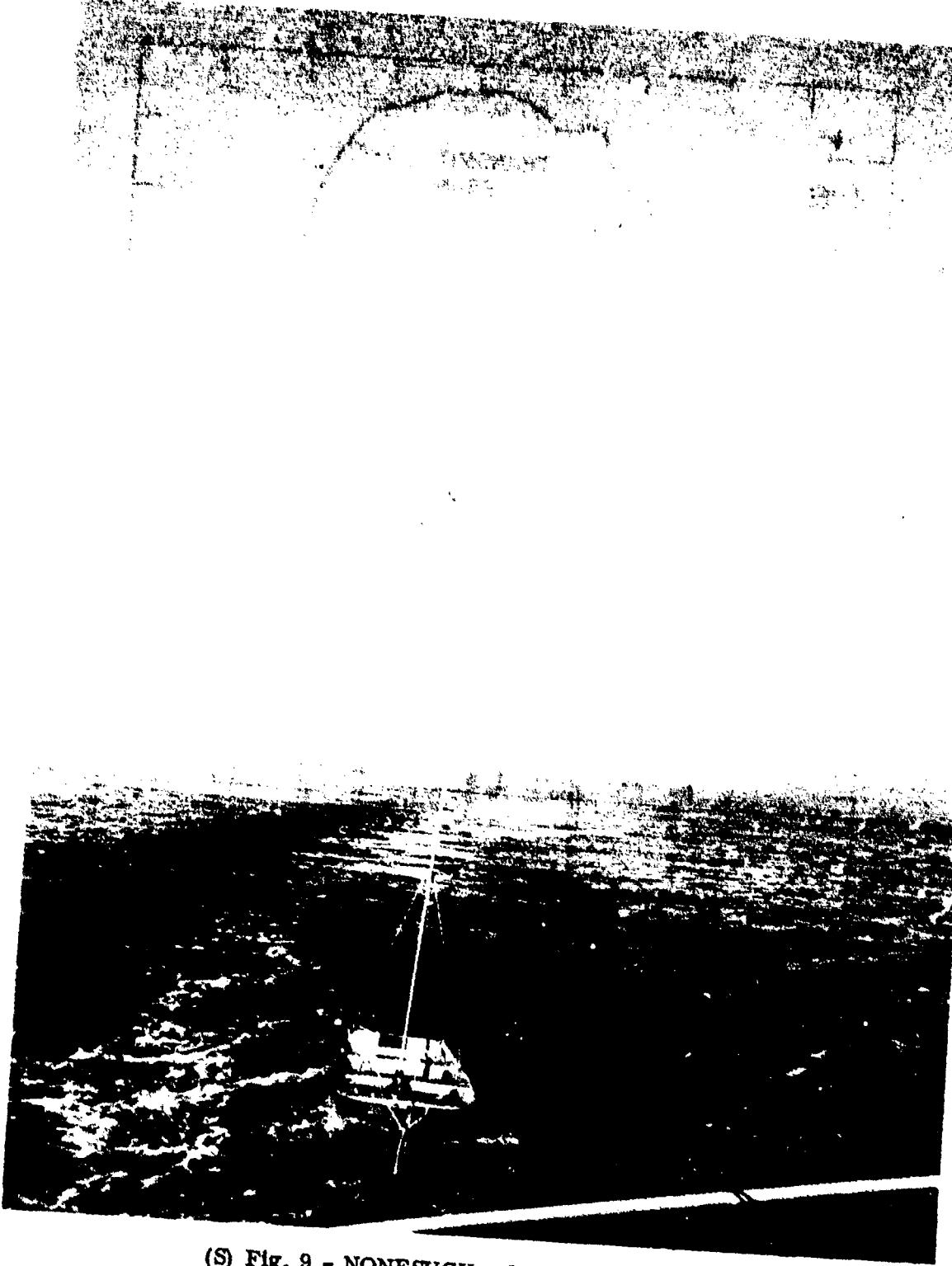
(S) Fig. 9 - NONESUCH calibration monopole
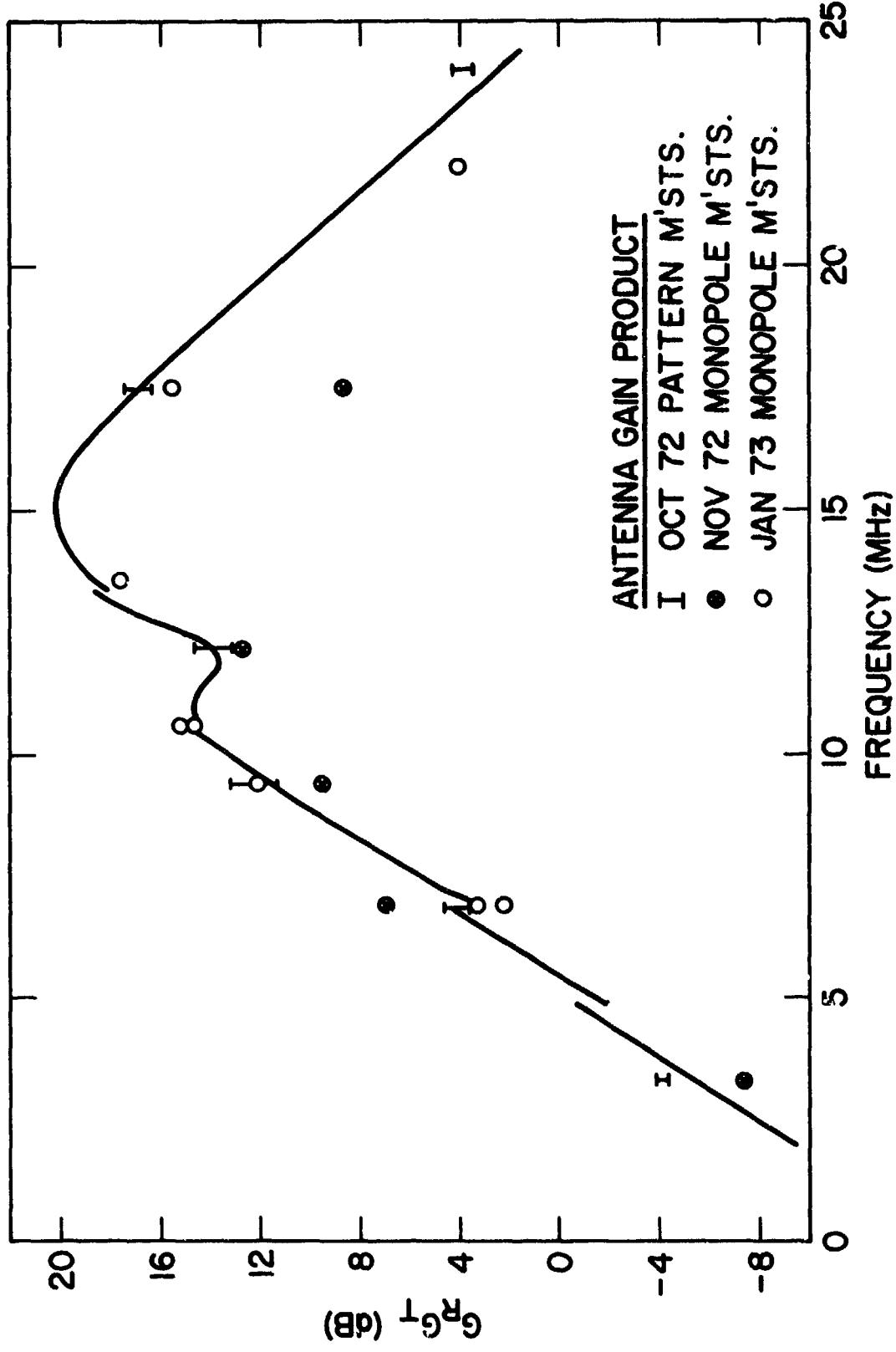
(S) Fig. 10 – Antenna gain product frequency dependence
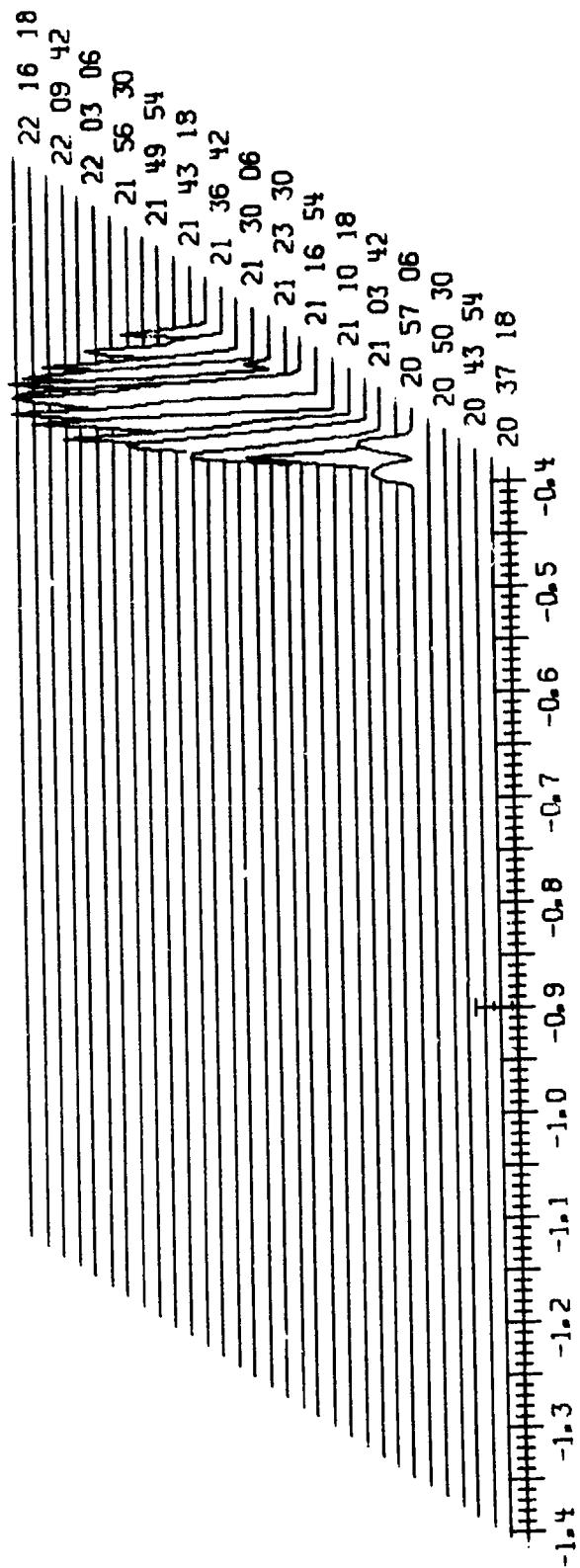
DOPPLER...HZ
FREQ 9.933 MHZ

DATE 12 07 72

(S) Fig. 11 – Isometric plot of effective boat cross-section at 9.933 MHz during transit of the range gate
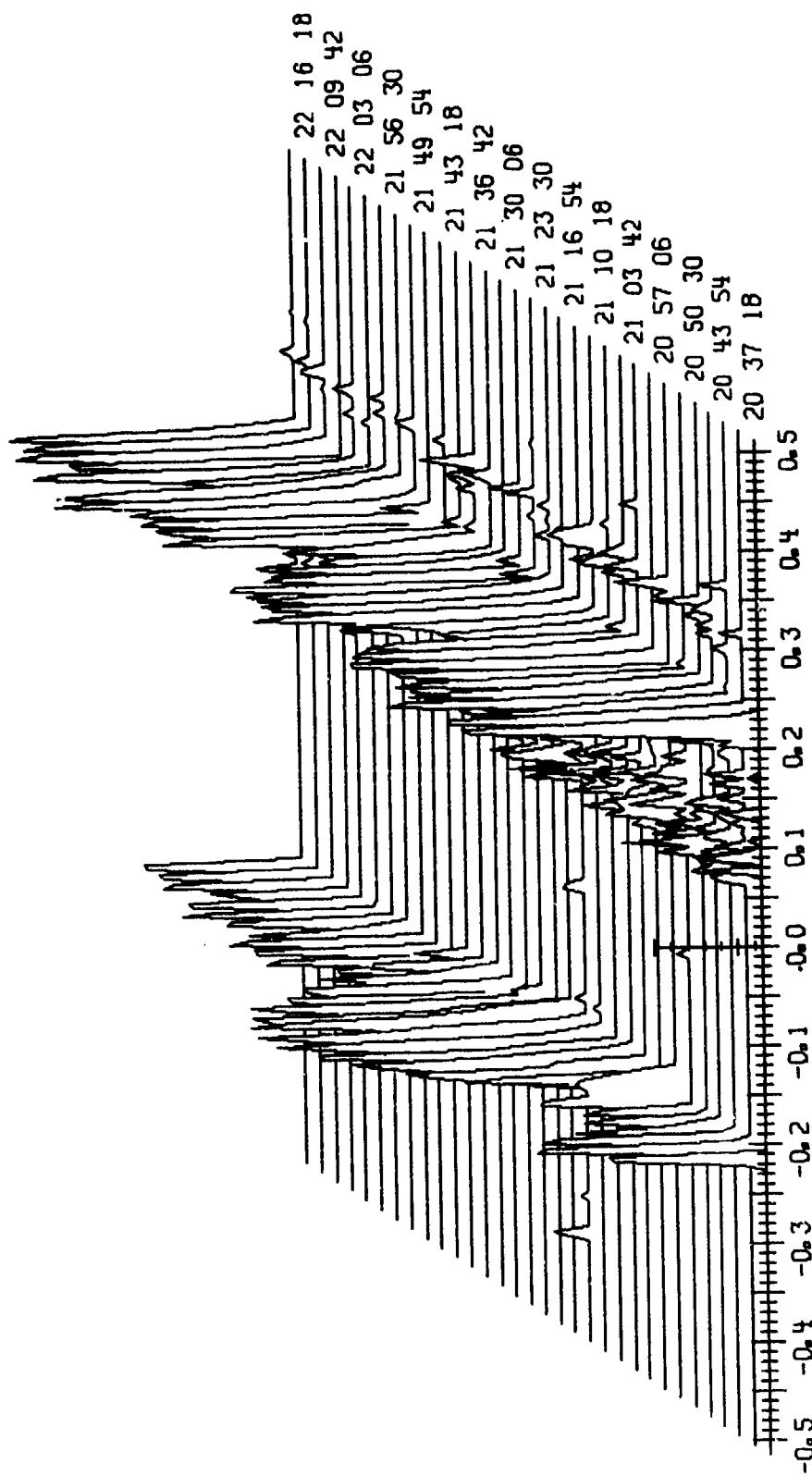
DOPPLER...HZ
FREQ 4.543 MHZ

DATE 12 07 72

(S) Fig. 12 – Sea-scatter versus doppler and time showing the recede and approach Bragg lines (4.543 MHz)

25

DOPPLER...HZ
FREQ 4.933 MHZ
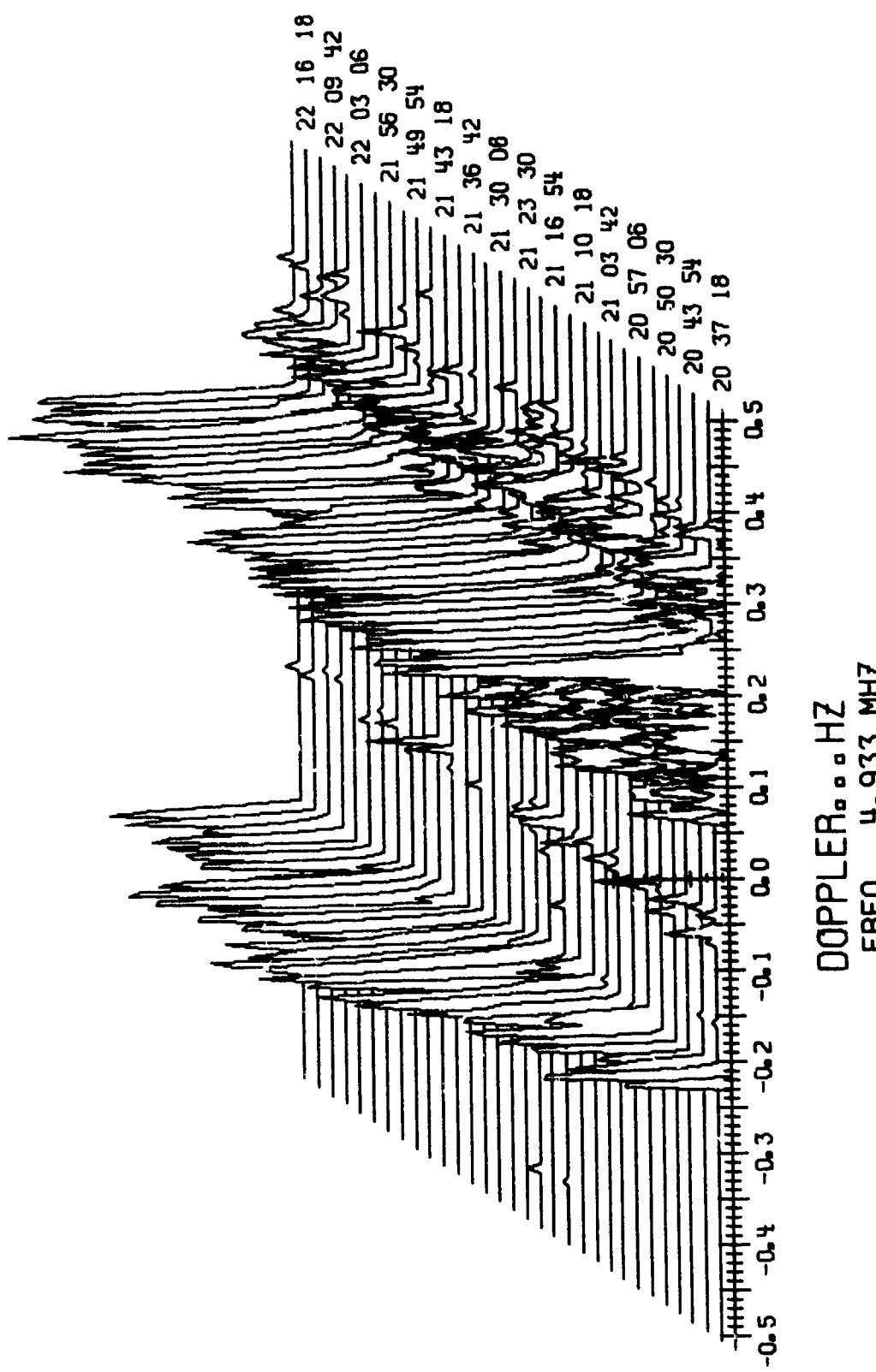
DATE 12 07 72

(S) Fig. 13 – Sea-scatter versus doppler and time showing the recede and approach Bragg lines (4.933 MHz)

DOPPLER...HZ
FREQ 5.033 MHZ
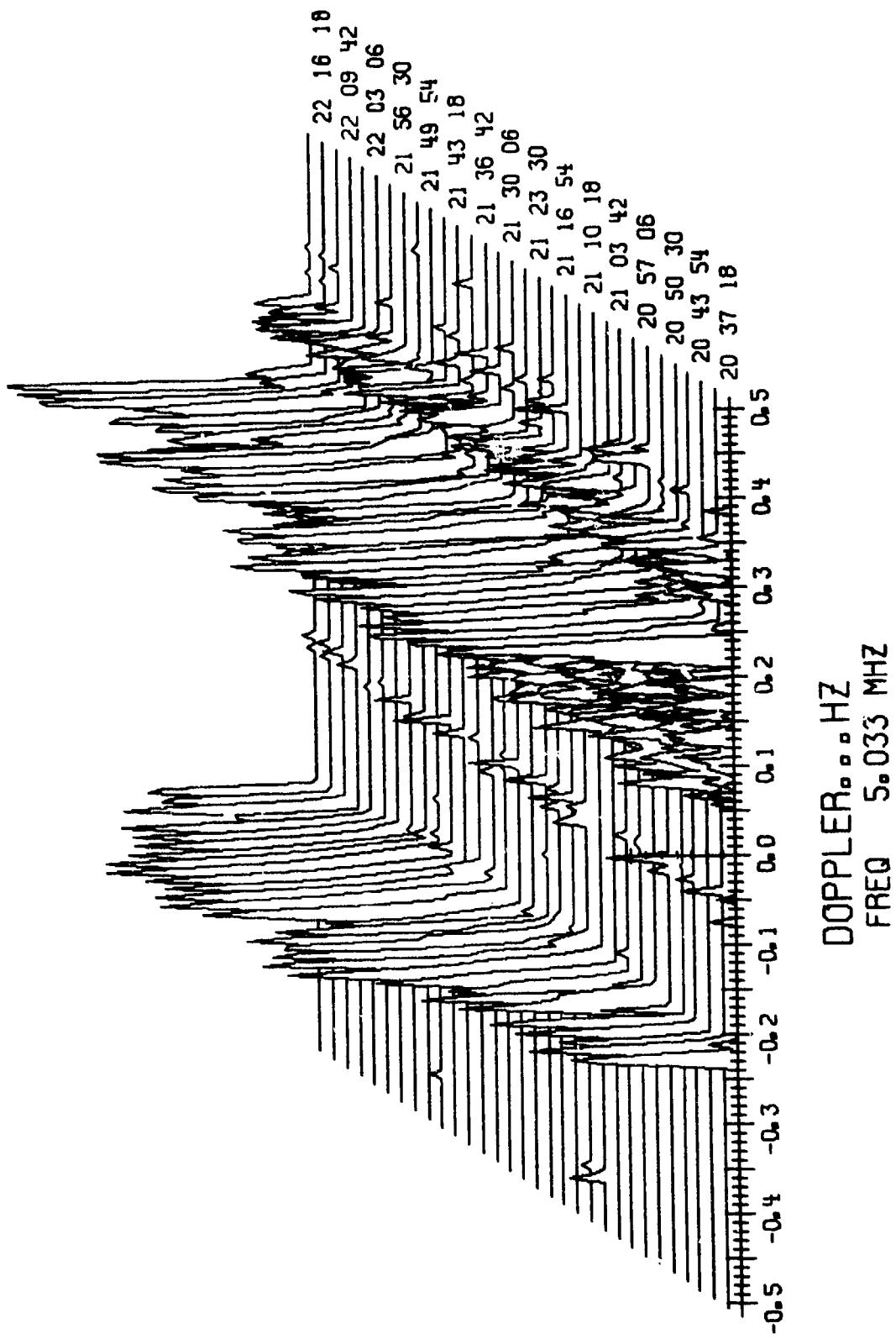
DATE 12 07 72

(S) Fig. 14 - Sea-scatter versus doppler and time showing the
recede and approach Bragg lines (5.033 MHz)

27

DOPPLER...HZ
FREQ 5.113 MHZ

DATE 12 07 72

(S) Fig. 15 - Sea-scatter versus doppler and time showing the recede and approach Bragg lines (5.113 MHz)
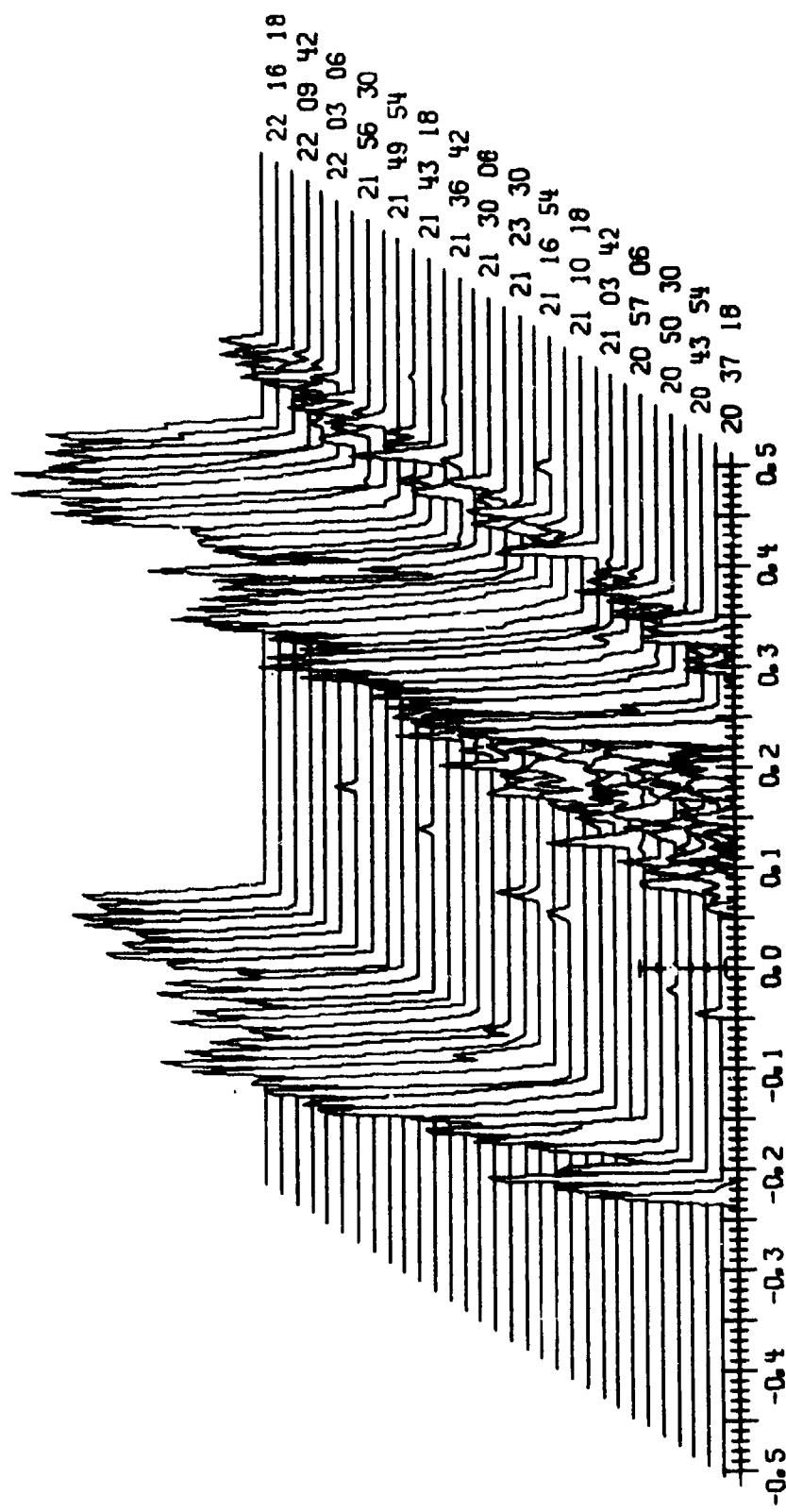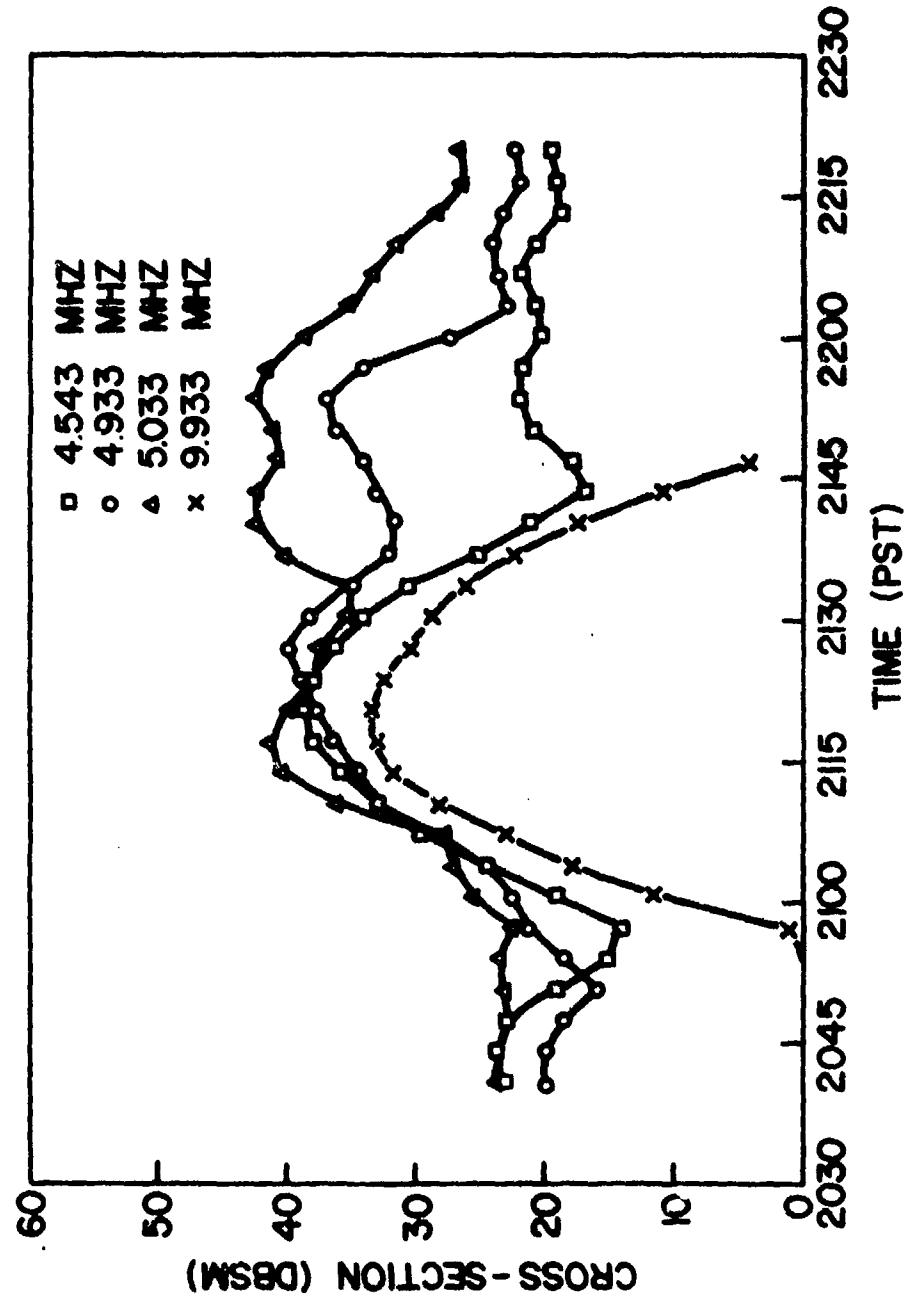
(S) Fig. 16 – Time profile of recede Bragg line intensity,
event of 7 December 1972

DOPPLER...HZ
FREQ 4.463 MHZ
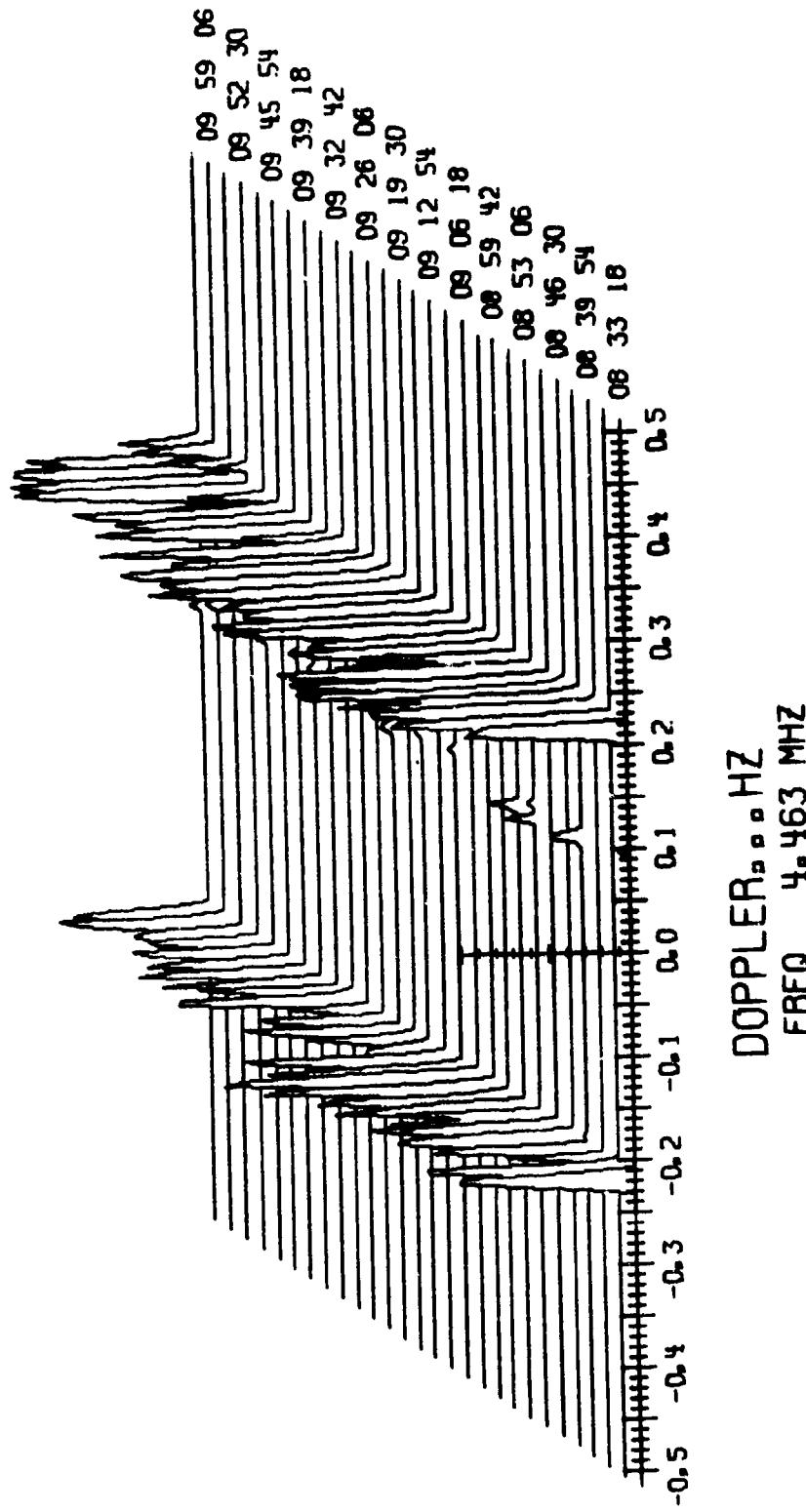
DATE 01 16 73

(S) Fig. 17 - Sea-scatter versus doppler and time showing the recede and approach Bragg lines (4.463 MHz)
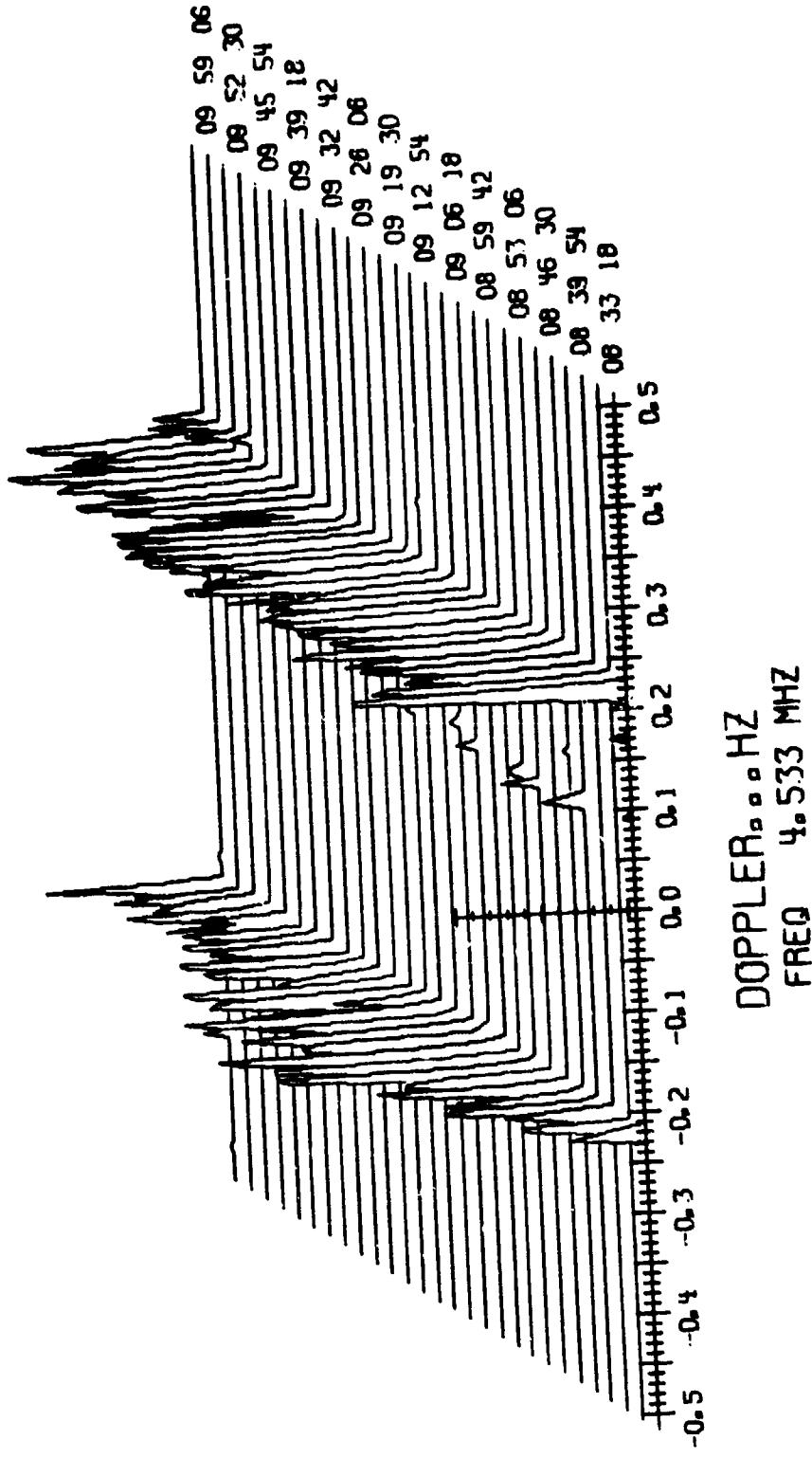
(S) Fig. 18 – Sea-scatter versus doppler and time showing the recede and approach Bragg lines (4.533 MHz)
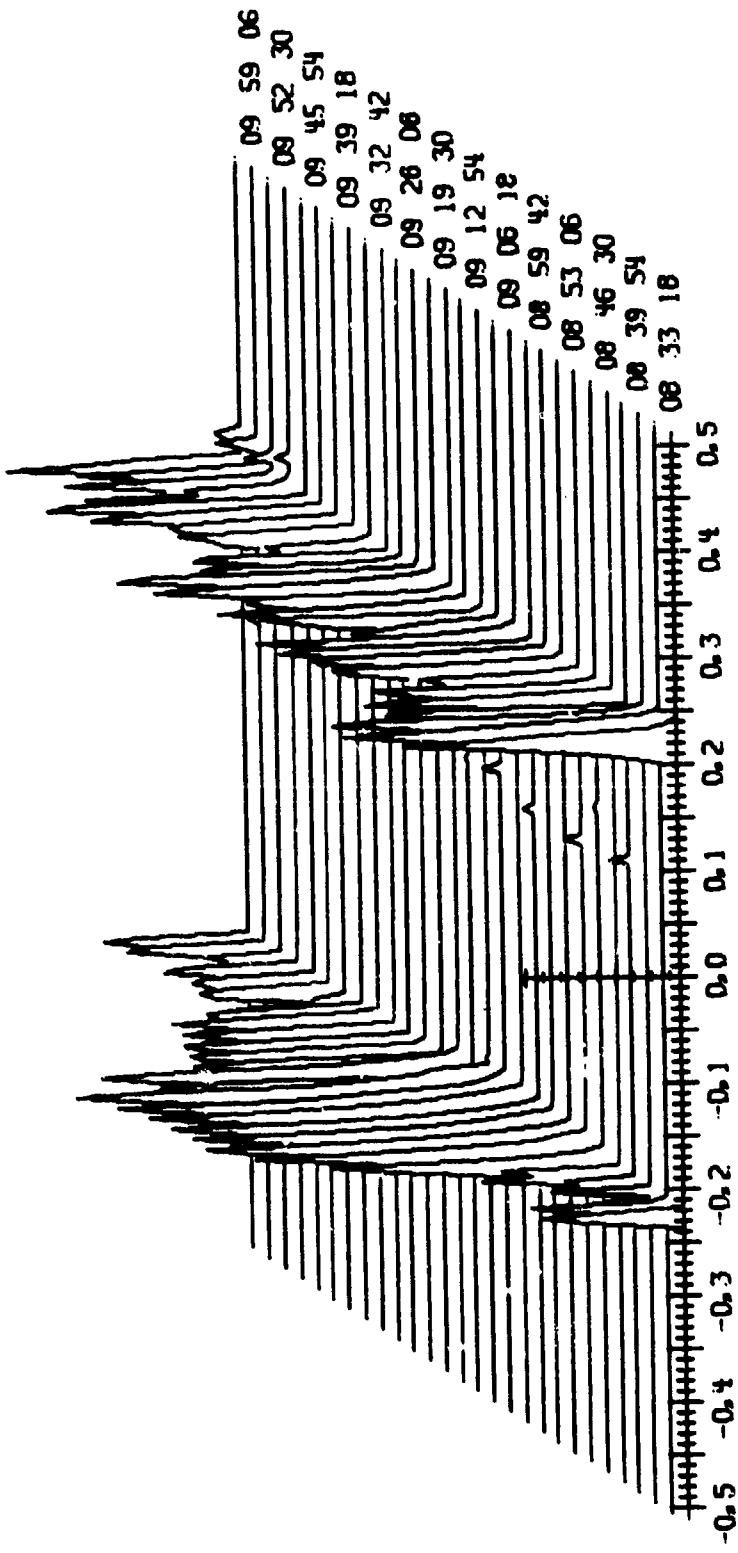
DOPPLER,,,HZ
FREQ 4.573 MHZ

DATE 01 16 73

(S) Fig. 19 – Sea-scatter versus doppler and time showing the recede and approach Bragg lines (4.573 MHz)

DOPPLER...HZ
FREQ   4.633 MHZ

DATE   01 16 73
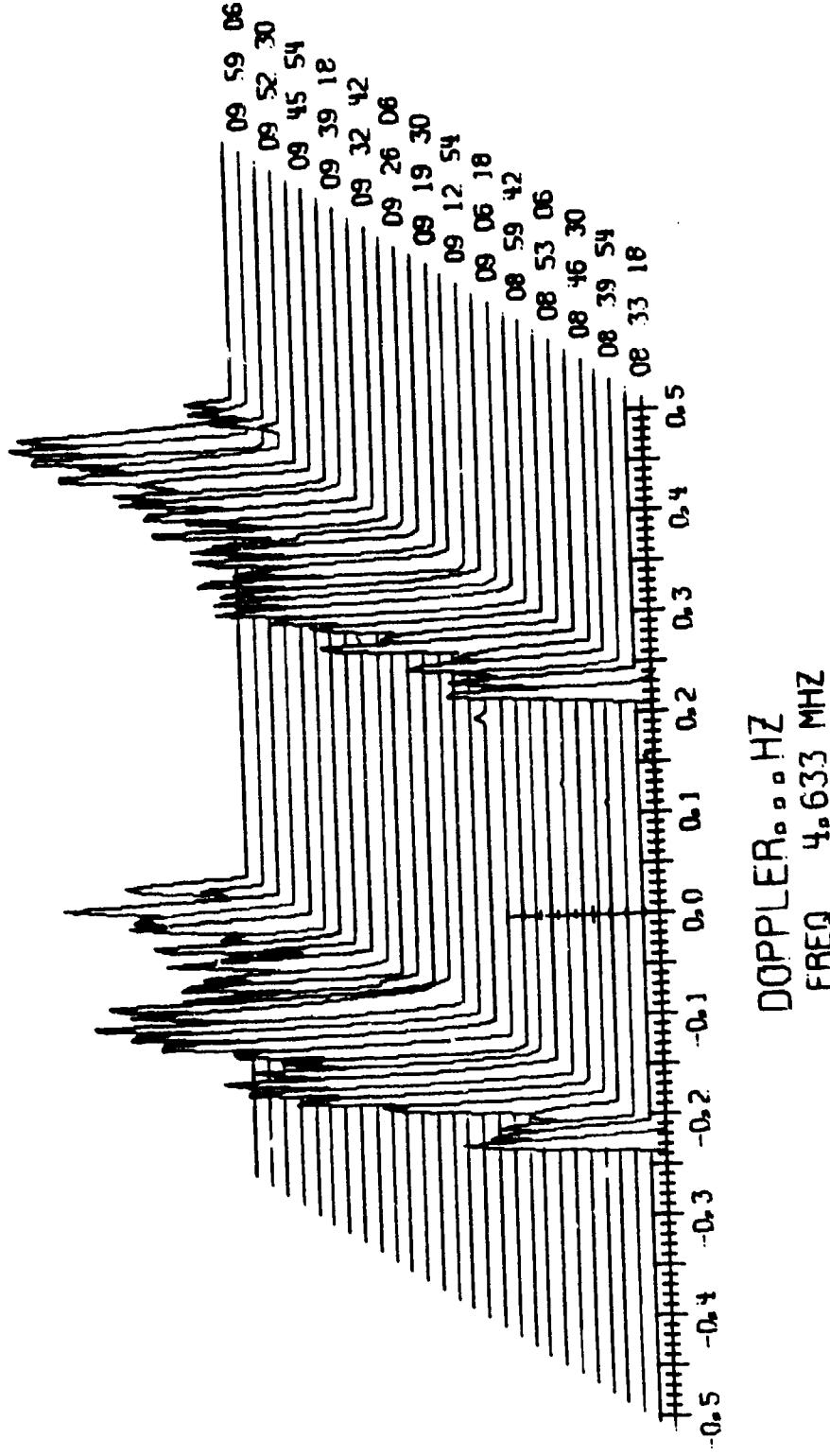
(S) Fig. 20 - Sea-scatter versus doppler and time showing the recede and approach Bragg lines (4.633 MHz)
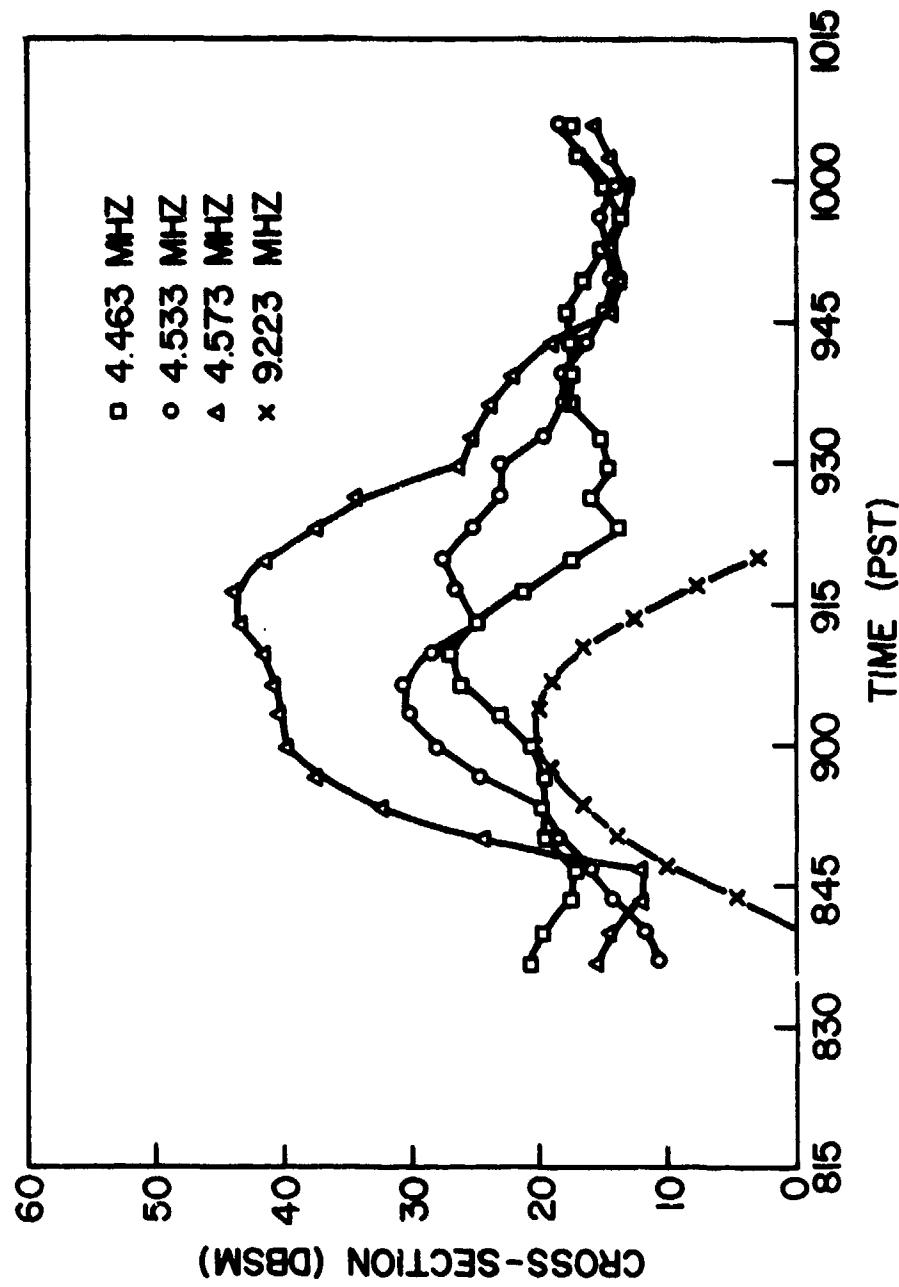
(S) Fig. 21 – Time profile of Bragg line intensity,
event of 16 January 1973

DOPP.ER, sec HZ
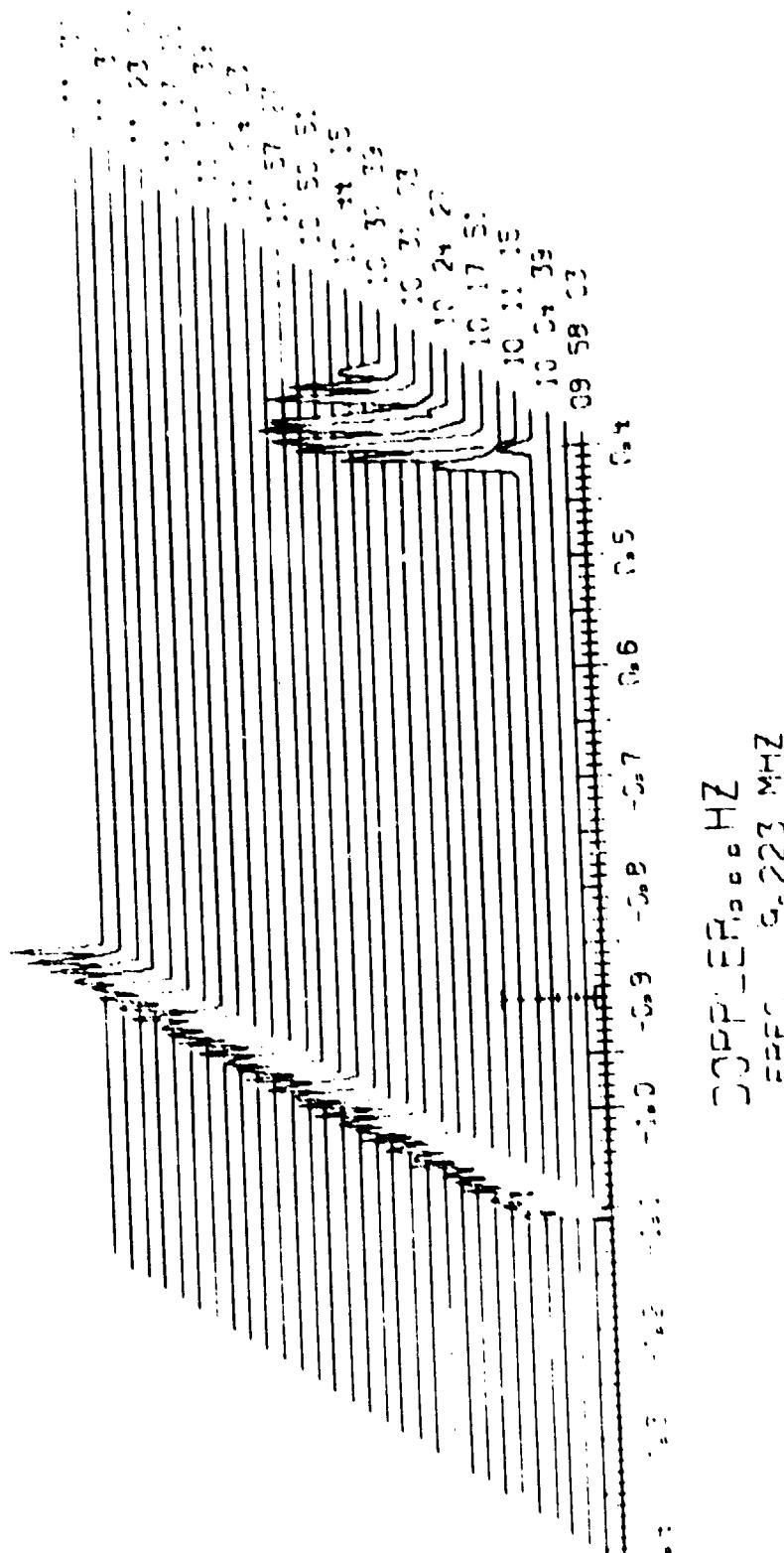
FREQ 9.223 MHZ

DATE 0, 15 73

(S) Fig. 22 – Isometric plot of effective boat cross-section at 9.223 MHz during transit of the range gate

DOPPLER...HZ
FREQ 4.463 MHZ

DATE 01 15 73
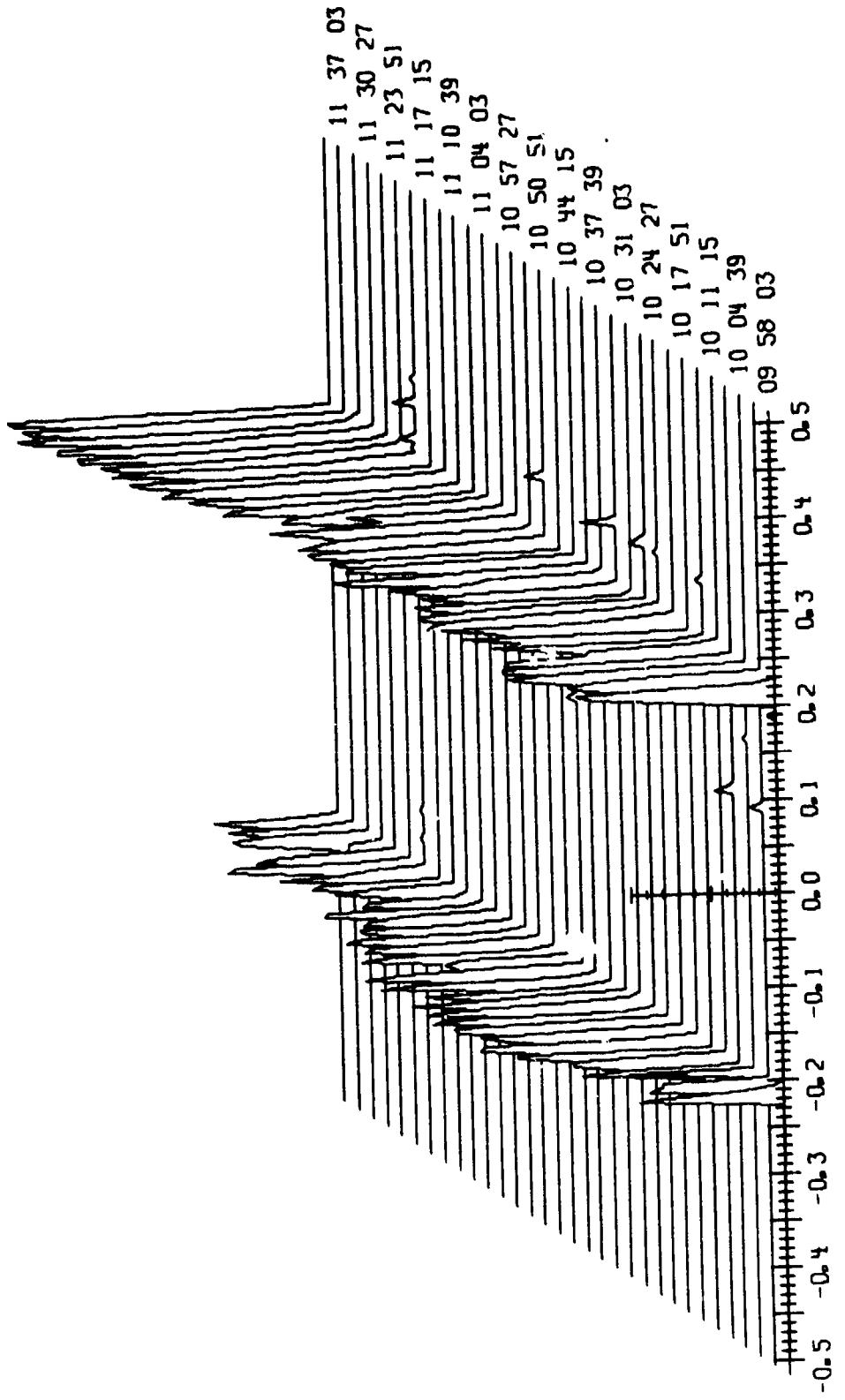
(S) Fig. 23 – Sea-scatter versus doppler and time showing the recede and approach Bragg lines (4.463 MHz)

36

DOPPLER...HZ
FREQ 4.573 MHZ
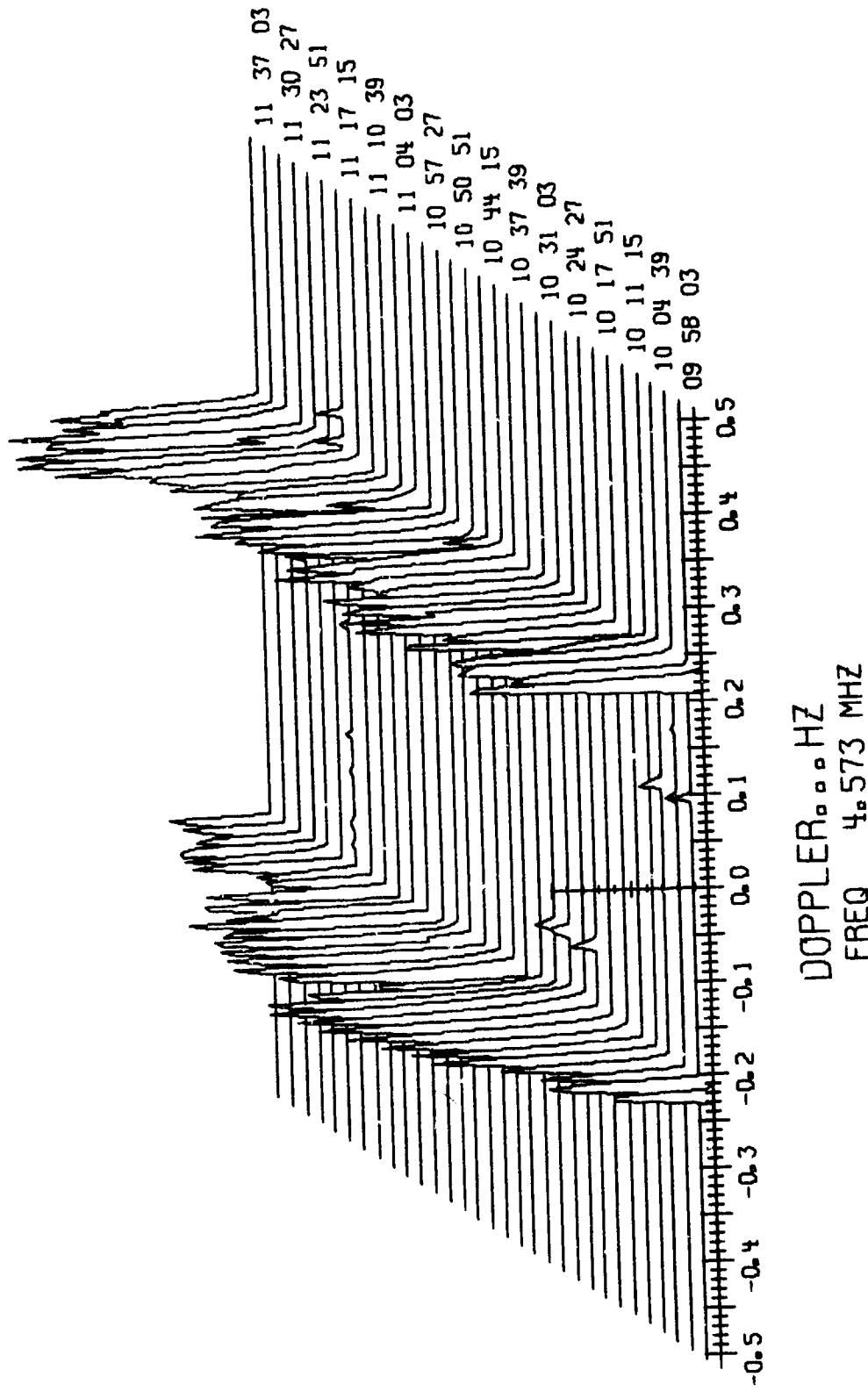
DATE 01 15 73

(S) Fig. 24 – Sea-scatter versus doppler and time showing the recede and approach Bragg lines (4.573 MHz)

DOPPLER...HZ
FREQ 4.773 MHZ
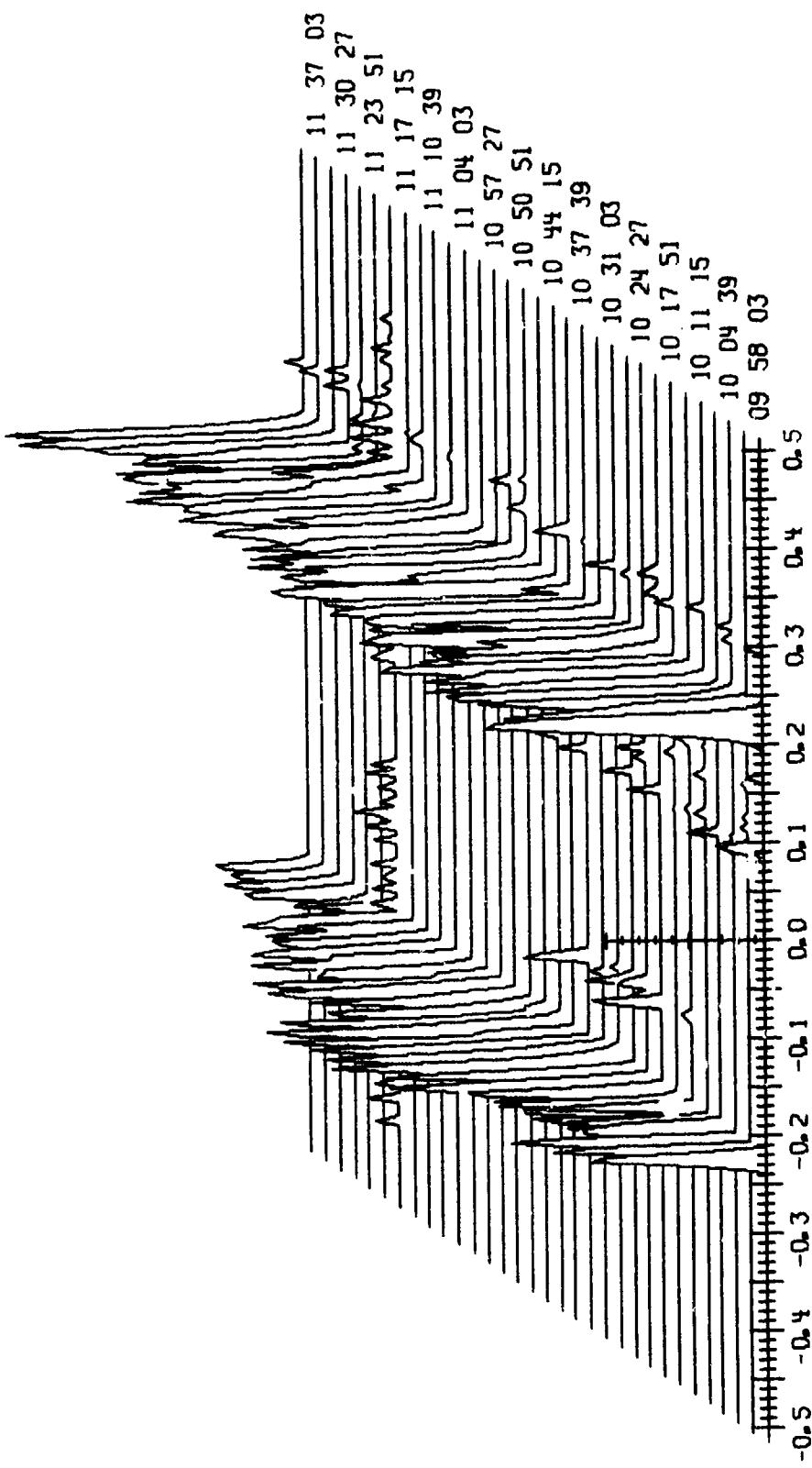
DATE 01 15 73

(S) Fig. 25 – Sea-scatter versus doppler and time showing the recede and approach Bragg lines (4.773 MHz)

DOPPLER₀₀₀HZ
FREQ 5.033 MHZ
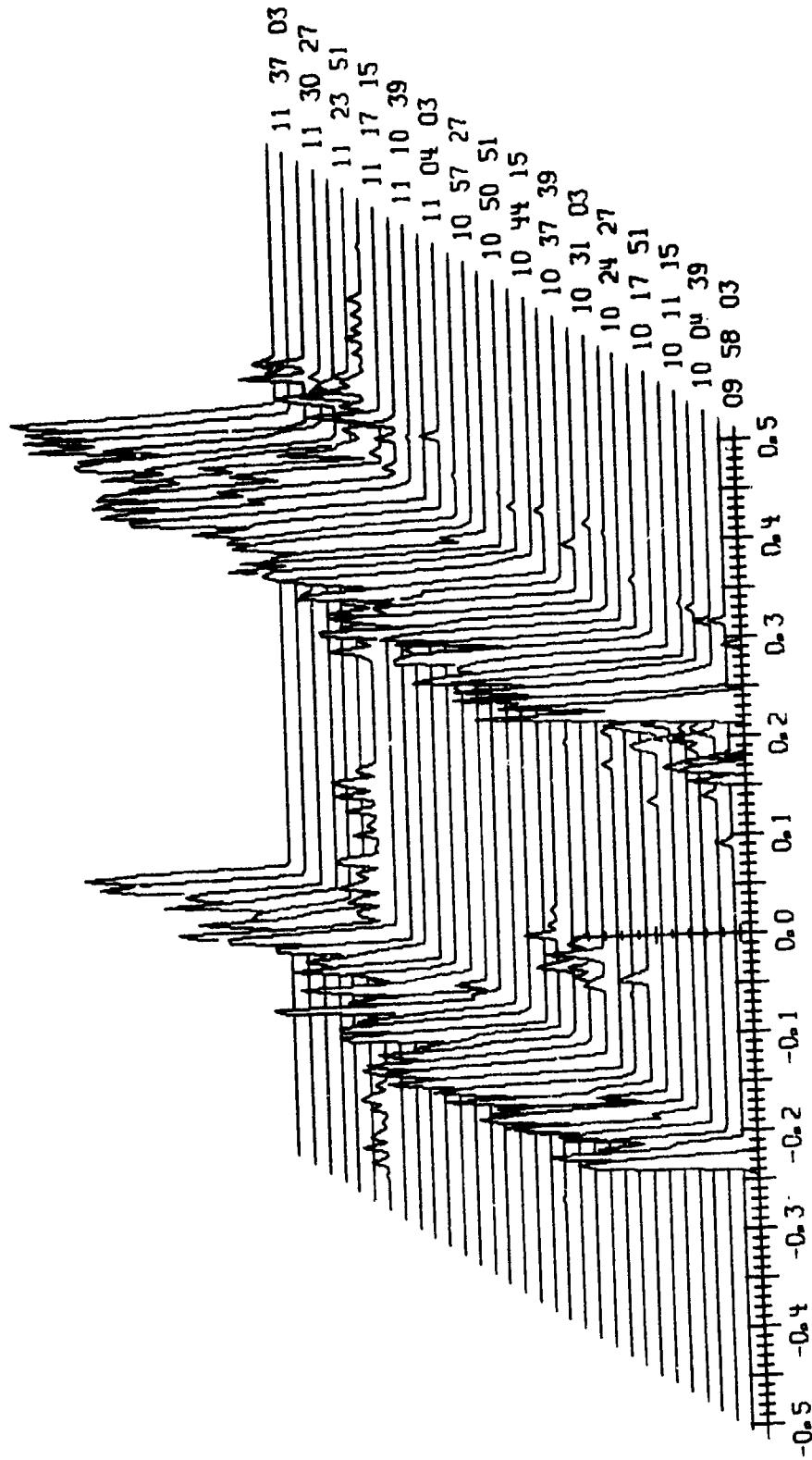
DATE 01 15 73

(S) Fig. 26 – Sea-scatter versus doppler and time showing the
recede and approach Bragg lines (5.033 MHz)

## DOCUMENT CONTROL DATA - R & D

(Security classification of title, body of abstract and indexing annotation must be entered when the overall report is classified)

1. ORIGINATING ACTIVITY *(Corporate author)*	2a. REPORT SECURITY CLASSIFICATION
Naval Research Laboratory Washington, D.C. 20375	SECRET-NOFORN
	2b. GROUP XGDS - 3 - 1993

3. REPORT TITLE

HF GROUND-WAVE BACKSCATTER FROM SURFACE TARGETS (U)
(Phase B - San Clemente Island)

4. DESCRIPTIVE NOTES *(Type of report and inclusive dates)*

A report on a continuing program.

5. AUTHOR(S) *(First name, middle initial, last name)*

Robert W. Bogle
Leonard S. Wagner

6. REPORT DATE	7a. TOTAL NO. OF PAGES	7b. NO. OF REFS
September 1973	44	26

8a. CONTRACT OR GRANT NO. NRL Problem - 53R02-87	9a. ORIGINATOR'S REPORT NUMBER(S)
b. PROJECT NO. RF12-151-402-4021	NRL Memorandum Report 2645
c. ARPA-1809	9b. OTHER REPORT NO(S) *(Any other numbers that may be assigned this report)*
d. XR021-05-003	

10. DISTRIBUTION STATEMENT

Distribution limited to U.S. Government Agencies only; test and evaluation, September 1973.
Other requests for this document must be referred to the Director, Naval Research
Laboratory, Washington, D.C. 20375.

11. SUPPLEMENTARY NOTES	12. SPONSORING MILITARY ACTIVITY
	Department of the Navy ARPA ONR & NAVELEX Washington, D.C. 20375

13. ABSTRACT

(SNF) Measurements of surface-vessel wakes have been made with an experimental
HF radar. The experimental program was conducted at San Clemente Island in deep
ocean areas. The radar was provided with considerable flexibility in frequency, range
and azimuth and an on-site digital processor was used to provide near real-time spectral
analyses. Preliminary results indicate that wakes are clearly distinguishable from the
clutter produced by a nominal sea. Examples are given. Analysis of effective wake
cross-section as a function of vessel speed and size and as a function of sea conditions
are proceeding.

DD FORM 1473 (PAGE 1)

S/N 0101-807-6801

14. KEY WORDS	LINK A		LINK B		LINK C	
	ROLE	WT	ROLE	WT	ROLE	WT
HF Radar						
OTH Radar						
Wakes						
Surface clutter						

MEMORANDUM

20 February 1997

Subj: Document Declassification

Ref: (1) Code 5309 Memorandum of 29 Jan. 1997
             (2) Distribution Statements for Technical Publications
                 NRL/PU/5230-95-293

Encl: (a) Code 5309 Memorandum of 29 Jan. 1997
             (b) List of old Code 5320 Reports
             (c) List of old Code 5320 Memorandum Reports

1. In Enclosure (a) it was recommended that the following reports be declassified,
four reports have been added to the original list:

Formal: 5589, 5811, 5824, 5825, 5849, 5862, 5875, 5881, 5903, 5962, 6015, 6079,
6148, 6198, 6272, 6371, 6476, 6479, 6485, 6507, 6508, 6568, 6590, 6611, 6731, 6866,
7044, 7051, 7059, 7350, 7428, 7500, 7638, 7655. Add 7684, 7692.

Memo: 1251, 1287, 1316, 1422, ████, 1500, 1527, 1537, 1540, 1567, 1637, 1647,
1727, 1758, 1787, 1789, 1790, 1811, 1817, 1823, 1885, 1939, 1981, 2135, 2624, 2701,
2645, 2721, 2722, 2723, 2766. Add 2265, 2715.

The recommended distribution statement for the these reports is: **Approved for
public release; distribution is unlimited.**

2. The above reports are included in the listings of enclosures (b) and (c) and
were selected because of familiarity with the contents. The rest of these documents
very likely should receive the same treatment.

J. M. Headrick
Code 5309

Copy:
     Code 1221 —— CR OK 7/9/97
     Code 5300
     Code 5320
     Code 5324